



U.S. Department of Energy
Pittsburgh Energy Technology Center

COAL LIQUEFACTION AND GAS CONVERSION

CONTRACTORS REVIEW CONFERENCE

PROCEEDINGS

VOLUME I

SEPTEMBER 27 - 29, 1993

Hyatt Regency Hotel
Pittsburgh, Pennsylvania

MASTER

DISTRIBUTION OF THIS DOCUMENT IS UNLIMITED

JFD

CONFERENCE COCHAIRPERSONS

S. Rogers, US Department of Energy/Pittsburgh Energy Technology Center

P. Zhou, Burns and Roe Services Corporation

SESSION CHAIRPERSONS

US Department of Energy/Pittsburgh Energy Technology Center

M.J. Baird

A.C. Bose

E.B. Klunder

S.C. Kornfeld

M.A. Nowak

V.U.S. Rao

G.J. Stiegel

Burns and Roe Services Corporation

J.J. Marano

R.D. Srivastava

P. Zhou

CONFERENCE STAFF

Center for Conference Management

N. Maceil

K. Lockhart

INVITED PLENARY SPEAKERS

M.M.G. Senden, Manager

Hydrocarbon Synthesis and Gasification

Shell Laboratories Amsterdam, The Netherlands

R.F. Bauman, Director

Synthetic Fuels Research

Exxon Research & Development Laboratories, USA

S.R. Drozda, Business Development Officer

U.S. Small Business Administration

Pittsburgh District Office

INVITED SESSION SPEAKERS

D.J. Allardice, Coal Corporation of Victoria, Australia

J. Erwin, Southwest Research Institute, USA

M.D. Gray, British Coal Liquefaction Project, UK

R.D. Hughes, British Coal Liquefaction Project, UK

K. Ikeda, Nippon Steel Corporation, Japan

S. Katsushima, New Energy & Industrial Technology Development Organization, Japan

T.J. Mazanec, BP America, USA

M.D. Reed, British Coal Liquefaction Project, UK

N. Robinson, British Coal Liquefaction Project, UK

INVITED PRESENTATION REVIEWERS

N.L. Carr, Consultant

D. Gray, MITRE

A.M. Hartstein, US Department of Energy/HQ

H.W. Haynes, Jr., University of Wyoming

R.F. Hickey, US Department of Energy/Pittsburgh Energy Technology Center

G.P. Holder, University of Pittsburgh

A.L. Lee, Institute of Gas Technology

T.J. Mazanec, BP America

H.G. McIlvried, Burns and Roe Services Corporation

R.R. Schehl, US Department of Energy/Pittsburgh Energy Technology Center

J. Shen, US Department of Energy/HQ

H.P. Stephens, Sandia National Laboratories

I. Wender, University of Pittsburgh

U.S. Department of Energy
Pittsburgh Energy Technology Center

COAL LIQUEFACTION AND GAS CONVERSION

CONTRACTORS' REVIEW CONFERENCE

September 27 - 29, 1993

**Hyatt Regency Hotel
Pittsburgh, Pennsylvania**

AGENDA



MONDAY, SEPTEMBER 27, 1993

**AR - COAL LIQUEFACTION
(Ballroom 1 & 2)**

Session Chairperson: V.U.S. Rao, Pittsburgh Energy Technology Center

- 8:30 - 8:40 a.m. Introductory Remarks**
- 8:40 - 9:10 a.m. Steam Pretreatment for Coal Liquefaction
R.A. Graff, The City College of New York**
- 9:10 - 9:40 a.m. The Dual Role of Oxygen Functions in Coal
Pretreatment and Liquefaction: Crosslinking
and Cleavage Reactions
M.A. Serio, Advanced Fuel Research, Inc.**
- 9:40 - 10:10 a.m. Technical and Economic Evaluation of a New Process
for Co-Liquefying Coal and Scrap Tires
M. El-Halwagi, Auburn University**
- 10:10 - 10:30 a.m. BREAK**
- 10:30 - 11:00 a.m. Chemistry of Catalytic Coal Liquefaction
B.C. Bockrath, Pittsburgh Energy Technology Center**
- 11:00 - 11:30 a.m. High Temperature/High Pressure ESR Spectroscopy
of Free Radicals in Coal Liquefaction, Coprocessing
and Catalyst Testing
M.M. Ibrahim, West Virginia University**

11:30a.m.-1:00p.m. LUNCH

afternoon session continued on next page

MONDAY, SEPTEMBER 27, 1993 (continued)

**AR-COAL LIQUEFACTION
(Ballroom 1 & 2)**

Session Chairperson: M. J. Baird, Pittsburgh Energy Technology Center

- 1:00 - 1:30 p.m. Dispersed Catalysts and Carbon-Based Catalysts for Direct Coal Liquefaction
M. Farcasiu, Pittsburgh Energy Technology Center**
- 1:30 - 2:00 p.m. New Approaches in the Synthesis and Characterization of Iron-Based Catalysts for Direct Coal Liquefaction
G.P. Huffman, University of Kentucky, CFFLS**
- 2:00 - 2:30 p.m. Clay-Supported Catalysts for Coal Liquefaction
E.S. Olson, Universal Fuel Development Associates, Inc.**
- 2:30 - 2:50 p.m. BREAK**
- 2:50 - 3:20 p.m. Activity Testing of Fine-Particle Size, Iron Catalysts for Coal Liquefaction
F.V. Stohl, Sandia National Laboratories**
- 3:20 - 4:30 p.m. Open Discussion - Catalyst Testing
Discussion Leader: M. J. Baird**

ADJOURN

MONDAY, SEPTEMBER 27, 1993

**GAS-TO-LIQUIDS
(Regency A)**

Session Chairperson: A.C. Bose, Pittsburgh Energy Technology Center

- 8:30 - 8:40 a.m. Introductory Remarks**
- 8:40 - 9:10 a.m. Development of Ceramic Membranes for Partial
Oxygenation of Hydrocarbon Fuels to High-Value-
Added Products
U. Balachandran, Argonne National Laboratory**
- 9:10 - 9:40 a.m. Oxidative Coupling of Methane using
Membrane Reactors
Y.H. Ma, Worcester Polytechnic Institute**
- 9:40 - 10:10 a.m. Electropox: BP's Novel Oxidation Technology
T.J. Mazanec, BP Chemicals**
- 10:10 - 10:30 a.m. BREAK**
- 10:30 - 11:00 a.m. Methyl Chloride via Oxyhydrochlorination of
Methane
B. Naasz, Dow Corning Corporation**
- 11:00 - 11:30 a.m. Exploratory Studies of Oxidative Conversion of
Methane to Methanol
C.E. Taylor, Pittsburgh Energy Technology Center**

11:30a.m. - 1:00p.m. LUNCH

afternoon session continued on next page

MONDAY, SEPTEMBER 27, 1993 (continued)

**GAS-TO-LIQUIDS
(Regency A)**

Session Chairperson: R. D. Srivastava, Burns and Roe Services Corp.

- 1:00 - 1:30 p.m. Conversion of Light Hydrocarbon Gases to Metal Carbides for Production of Liquid Fuels and Chemicals
W.A. Peters, Massachusetts Institute of Technology**
- 1:30 - 2:00 p.m. Light Hydrocarbon Gas Conversion using Halogenated Iron Dodecaphenylporphyrin Catalysts
J. A. Shelnutt, Sandia National Laboratories**
- 2:00 - 2:30 p.m. Novel Catalysts for Methane Activation
R. Malhotra, SRI International**
- 2:30 - 2:50 p.m. BREAK**
- 2:50 - 3:20 p.m. Development of Vanadium-Phosphate Catalysts for Methane Partial Oxidation
R.L. McCormick, Amax Research & Development Center**
- 3:20 - 3:50 p.m. Direct Aromatization of Methane
G. Marcelin, Altamira Instruments, Inc.**

ADJOURN

TUESDAY, SEPTEMBER 28, 1993

**PLENARY SESSION
(Ballroom 4)**

- 8:30 - 8:45 a.m. Welcome and Introductory Remarks
G. V. McGurl,
Pittsburgh Energy Technology Center
- 8:45 - 9:15 a.m. DOE Keynote Address
G. V. McGurl
Pittsburgh Energy Technology Center
- 9:15 - 9:55 a.m. Plenary Speaker
M.M.G. Senden, Koninklijke/Shell Laboratorium
Amsterdam, The Netherlands
- 9:55 - 10:15 a.m. BREAK
- 10:15 - 10:55 a.m. Plenary Speaker
R.F. Bauman, EXXON Research &
Development Laboratories
- 10:55 - 11:10 a.m. S.R. Drozda
U.S. Small Business Administration
District Office/Pittsburgh

SESSIONS CONTINUED ON NEXT PAGE

TUESDAY, SEPTEMBER 28, 1993

**DIRECT LIQUEFACTION
(Regency B)**

Session Co-Chairpersons:

S. C. Kornfeld and M. A. Nowak, Pittsburgh Energy Technology Center

**11:15 - 11:45 a.m. Proof of Concept Facility for Direct Liquefaction
A.G. Comolli, Hydrocarbon Research Inc.**

**11:45 a.m. - 12:15 p.m. Direct Coal Liquefaction - Capital Cost and
Economics for Improved Baseline Design
S.K. Poddar, Bechtel Corporation**

12:15 - 1:45 p.m. LUNCH

**1:45 - 2:15 p.m. Improved Coal Liquefaction through
Enhanced Recycle Distillate Quality
F. J. Derbyshire, Center for Applied Energy Research,
University of Kentucky**

**2:15 - 2:45 p.m. Advanced Liquefaction Using Coal Swelling and
Catalyst Dispersion
D.C. Cronauer, Amoco Oil Company**

**2:45 - 3:15 p.m. Application of Carbon Monoxide/Steam and
Counterflow Reactor Technologies to Coal
Liquefaction
P.L. Simpson, Alberta Research Council
D. J. Berger, Canadian Energy Developments Inc.**

3:15 - 3:30 p.m. BREAK

**3:30 - 4:00 p.m. Highly Dispersed Catalysts for Coal Liquefaction
A. S. Hirschon, SRI International**

**4:00 - 4:30 p.m. Advanced Concepts in Coal Liquefaction -
Optimization of Reactor Configuration in
Coal Liquefaction
V. R. Pradhan, Hydrocarbon Research Inc.**

**4:30 - 5:00 p.m. Coal Liquefaction Process Streams Characterization
and Evaluation
S.D. Brandes, CONSOL, Inc.**

ADJOURN

TUESDAY, SEPTEMBER 28, 1993

**INDIRECT LIQUEFACTION (Oxygenated Fuels)
(Ballroom 2)**

Session Co-Chairpersons:

G.J. Stiegel, Pittsburgh Energy Technology Center

R.D. Srivastava, Burns and Roe Services Corp.

- 11:15 - 11:45 a.m. Heterogeneous Catalytic Process for Alcohol Fuels from Syngas
D.M. Minahan, Union Carbide Chemicals & Plastics Co., Inc.**
- 11:45 a.m. - 12:15 p.m. The Economical Production of Alcohol Fuels from Coal-Derived Synthesis Gas
W.B. Whiting, West Virginia University**
- 12:15 - 1:45 p.m. LUNCH**
- 1:45 - 2:15 p.m. Isobutanol Dehydration: A Key Step in Producing MTBE from Syngas
B.A. Toseland, Air Products and Chemicals, Inc.**
- 2:15 - 2:45 p.m. High Octane Ethers from Synthesis Gas-Derived Alcohols
K. Klier, Lehigh University**
- 2:45 - 3:15 p.m. Progress on Developing Technology for Producing Higher Alcohols from Syngas
G. W. Roberts, North Carolina State University**
- 3:15 - 3:30 p.m. BREAK**
- 3:30 - 4:00 p.m. Development of Alternative Fuels from Synthesis Gas
D.M. Brown, Air Products and Chemicals, Inc.**
- 4:00 - 4:30 p.m. Catalysts and Process Development for Synthesis Gas Conversion to Isobutylene
R. G. Anthony, Texas A&M University**

ADJOURN

WEDNESDAY, SEPTEMBER 29, 1993

DIRECT LIQUEFACTION

(Regency B)

Session Co-Chairpersons:

E. B. Klunder and M. J. Baird, Pittsburgh Energy Technology Center

**8:30 - 9:00 a.m. The Effect of Dispersed Catalysts on First Stage
Coal Liquefaction
A.V. Cugini, Pittsburgh Energy Technology Center**

**9:00 - 9:30 a.m. Conceptual Design & Economic Evaluation of BCL
Project
S. Katsushima, New Energy and Industrial
Technology Development Organization, Japan**

**9:00 - 10:00 a.m. Liquefaction Studies on Victorian Brown Coal
D.J. Allardice, Coal Corporation of Victoria,
Australia**

10:00 - 10:20 a.m. BREAK

**10:20 - 11:20 a.m. M.D. Gray, M.D. Reed, R.D. Hughes, N. Robinson
British Coal Corporation, UK**

**10:50 - 11:20 a.m. Liquefaction Characteristics of Wyoming Coal
K. Ikeda, Nippon Steel Corporation, Japan**

11:50 a.m. - 1:20 p.m. LUNCH

afternoon session continued on next page

WEDNESDAY, SEPTEMBER 29, 1993 (continued)

DIRECT LIQUEFACTION

(Regency B)

Session Chairperson:

P. Zhou, Burns and Roe Services Corp.

- 1:20 - 1:50 p.m. Catalytic Multi-Stage Liquefaction of Coal
L.K.T. Lee, Hydrocarbon Research, Inc.**
- 1:50 - 2:20 p.m. Effects of Low-Temperature Catalytic
Pretreatments on Coal Structure and Reactivity
in Liquefaction
C. Song, The Pennsylvania State University**
- 2:20 - 2:50 p.m. The Effects of Different Drying Processes on Coal
Liquefaction Yields
F.P. Miknis, Western Research Institute**
- 2:50 - 3:10 p.m. BREAK**
- 3:10 - 3:40 p.m. Mitigating Crosslinking Reactions through
Preconversion Strategies
D.F. McMillen, SRI International**
- 3:40 - 4:10 p.m. Surfactant-Assisted Coal Liquefaction at Milder
Processing Conditions
P.K. Sharma and G.S. Hickey
California Institute of Technology**
- 4:10 - 4:40 p.m. New Direction to Preconversion Processing of Coal
M. Nishioka, Viking Systems International**

ADJOURN

WEDNESDAY, SEPTEMBER 29, 1993

**INDIRECT LIQUEFACTION
(FISCHER-TROPSCH TECHNOLOGY)
(Ballroom 2)**

Session Chairperson:

V.U.S. Rao, Pittsburgh Energy Technology Center

**8:30 - 9:30 a.m. Technology Development for Cobalt Fischer-Tropsch Catalysts
A. H. Singleton, Energy International Corporation**

**9:00 - 9:30 a.m. Fischer-Tropsch Co/Ru Catalyst Development
R. R. Frame, UOP**

**9:30 - 10:00 a.m. Technology Development for Iron Fischer-Tropsch Catalysts
B. H. Davis, Center for Applied Energy Research, University of Kentucky, CAER**

10:00 - 10:20 a.m. BREAK

**10:20 - 10:50 a.m. Fischer-Tropsch Iron Catalyst Development
R.R. Frame, UOP**

**10:50 - 11:20 a.m. Development of Improved Iron Fischer-Tropsch Catalysts
D. B. Bukur, Texas A&M University**

**11:20 - 11:50 a.m. Mossbauer Spectroscopy Study of Iron-Based Catalysts Used in Fischer-Tropsch Synthesis
K.R.P.M. Rao, University of Kentucky, CFFLS**

11:50 a.m. - 1:20 p.m. LUNCH

afternoon session continued on next page

WEDNESDAY, SEPTEMBER 29, 1993 (continued)

**INDIRECT LIQUEFACTION
(FISCHER-TROPSCH TECHNOLOGY)
(Ballroom 2)**

Session Chairperson:

J.J. Marano, Burns and Roe Services Corp.

- 1:20 - 1:50 p.m. The Selective Catalytic Cracking of Fischer-Tropsch Liquids to High Value Transportation Fuels
W.J. Reagan, Amoco Oil Company**
- 1:50 - 2:20 p.m. The Standing of Fischer-Tropsch Diesel in an Assay of Fuel Performance and Emissions
J. Erwin, Southwest Research Institute**
- 2:20 - 2:50 p.m. Baseline Design/Economics for Advanced Fischer-Tropsch Technology
S. S. Tam, Bechtel Corporation**
- 2:50 - 3:10 p.m. BREAK**
- 3:10 - 3:40 p.m. Opportunities for Reducing Product Costs in Indirect Liquefaction
D. Gray, The MITRE Corporation**
- 3:40 - 4:10 p.m. Fischer-Tropsch Slurry Reactor Modeling
Y. Soong, Pittsburgh Energy Technology Center**

ADJOURN

TABLE OF CONTENTS

VOLUME I

AR - COAL LIQUEFACTION

STEAM PRETREATMENT FOR COAL LIQUEFACTION

Graff, R.A.; Balogh-Nair, V.; Ivanenko, O.; and Brathwaite, C.
The City College of New York 1

THE DUAL ROLE OF OXYGEN FUNCTIONS IN COAL PRETREATMENT AND LIQUEFACTION: CROSSLINKING AND CLEAVAGE REACTIONS

Serio, M.A.; Kroo, E.; Charpenay, S.; Solomon, P.R.; and Bassilakis, R.
Advanced Fuel Research, Inc.
McMillen, D.F.; Malhotra, R.; Satyam, A.; and Manion, J.
SRI International 15

TECHNICAL AND ECONOMIC EVALUATION OF A NEW PROCESS FOR CO-LIQUEFYING COAL AND SCRAP TIRES

Warren, A., and El-Halwagi, M.
Auburn University 45

CHEMISTRY OF CATALYTIC COAL LIQUEFACTION

Bockrath, B.; Illig, E.; Keller III, M.; Schroeder, K.; Bittner, E.; and Solar, J.
Pittsburgh Energy Technology Center 71

HIGH TEMPERATURE/HIGH PRESSURE ESR SPECTROSCOPY OF FREE RADICALS IN COAL LIQUEFACTION, COPROCESSING AND CATALYST TESTING

Seehra, M.S., and Ibrahim, M.M.
West Virginia University 85

SYNTHESIS AND CHARACTERIZATION OF NOVEL IRON-BASED CATALYSTS FOR DIRECT COAL LIQUEFACTION

Taghiei, M. M.; Zhao, J.; Feng, Z.; Rao, K.R.P.M.; Huggins, F.E.; and Huffman, G.P.
University of Kentucky, CFFLS 87

CLAY-SUPPORTED CATALYSTS FOR COAL LIQUEFACTION

Sharma, R.K., and Stanley, D.C.
University of North Dakota Energy & Environmental Research Center
Olson, E.S.; Buchwitz, C.M.; and Yagelowich, M.L.
Universal Fuel Development Associates, Inc. 105

ACTIVITY TESTING OF FINE-PARTICLE SIZE, IRON CATALYSTS FOR COAL LIQUEFACTION

Stohl, F.V.; Diegert, K.V.; and Gugliotta, T.P.
Sandia National Laboratories 123

GAS-TO-LIQUIDS

DEVELOPMENT OF CERAMIC MEMBRANES FOR PARTIAL OXYGENATION OF HYDROCARBON FUELS TO HIGH-VALUE-ADDED PRODUCTS

Balachandran, U.; Morissette, S.L.; Dusek, J.T.; Poeppel, R.B. and Mieville, R.L.
Argonne National Laboratory
Kleefisch, M.S.; Kobylinski, T.P.; Udovich, C.A.; and Pei, S.
Amoco Research Center 137

OXIDATIVE COUPLING OF METHANE USING INORGANIC MEMBRANE REACTOR

Ma, Y.H.; Moser, W.R.; Dixon, A.G.; Ramachandra, A.M.; Boye, A.; and Lu, Y.
Worcester Polytechnic Institute 161

METHYL CHLORIDE VIA OXYHYDROCHLORINATION OF METHANE

Naasz, B.M.; Smith, J.S.; Ferguson, S.P.; Knutson, C.G.; and Jarvis, R.F.
Dow Corning Corporation 193

EXPLORATORY STUDIES OF OXIDATIVE CONVERSION OF METHANE TO METHANOL

Taylor, C.E.; Anderson, R.R.; White, C.M.; and Noceti, R.P.
Pittsburgh Energy Technology Center 215

CONVERSION OF LIGHT HYDROCARBON GASES TO METAL CARBIDES FOR PRODUCTION OF LIQUID FUELS AND CHEMICALS

Diaz, A.F.; Modestino, A.J.; Chung, M.K.; Howard, J.B.; Tester, J.W.;
and Peters, W.A.
Massachusetts Institute of Technology 225

**LIGHT HYDROCARBON GAS CONVERSION USING HALOGENATED IRON
DODECAPHENYLPORPHYRIN CATALYSTS**

Showalter, M.; Erkkila, K.; and Shelnut, J.A.
Sandia National Laboratories 249

FULLERENE-BASED CATALYSTS FOR METHANE ACTIVATION

Hirschon, A.S.; Malhotra, R.; Wilson, R.B.; and Wu, H-J.
SRI International 265

**DEVELOPMENT OF VANADIUM-PHOSPHATE CATALYSTS FOR METHANE
PARTIAL OXIDATION**

McCormick, R.L.; Jha, M.C.; and Streuber, R.D.
Amax Research & Development Center 277

DIRECT AROMATIZATION OF METHANE

Marcelin, G.; Oukaci, R.; and Migone, R.A.
Altamira Instruments, Inc. 299

DIRECT LIQUEFACTION

PROOF OF CONCEPT FACILITY FOR DIRECT LIQUEFACTION

Comolli, A.G.; Lee, L.K.; Pradhan, V.R.; and Statzer, R.H.
Hydrocarbon Research Inc. 319

**DIRECT COAL LIQUEFACTION—CAPITAL COST AND ECONOMICS
FOR IMPROVED BASELINE DESIGN**

Poddar, S.K.
Bechtel Corporation
Kramer, S.J.
Amoco Oil Company
Basu, A.
Amoco Chemical Company 333

**IMPROVED COAL LIQUEFACTION THROUGH ENHANCED RECYCLE
DISTILLATE QUALITY**

Derbyshire, F., and Givens, E.
University of Kentucky/CAER
Burke, F.; Winschel, R.; and Lancet, M.
CONSOL Inc.
Stephens, H., and Kottenstette, R.
Sandia National Laboratories
Peluso, M.
LDP Associates 353

**ADVANCED LIQUEFACTION USING COAL SWELLING AND CATALYST
DISPERSION**

Cronauer, D.C., and Torres-Ordonez, R.J.
Amoco Oil Company
Curtis, C.W.
Auburn University
Chander, S.
The Pennsylvania State University
Gutterman, C.
Foster Wheeler Development Corporation 379

**APPLICATION OF CARBON MONOXIDE/STEAM AND COUNTERFLOW
REACTOR TECHNOLOGIES TO COAL LIQUEFACTION**

Berger, D.J.
Canadian Energy Developments Inc.
Simpson, P.L., and Parker, R.J.
Alberta Research Council 397

INVESTIGATION OF ADVANCED LIQUEFACTION CONCEPTS

Hirschon, A.S.; Wilson, R.B.; and Kim, S.
SRI International 417

**ADVANCED CONCEPTS IN COAL LIQUEFACTION-OPTIMIZATION OF
REACTOR CONFIGURATION IN COAL LIQUEFACTION**

Pradhan, V.R.; Comolli, A.G.; Johanson, E.S.; Lee, L.K.; and Stalzer, R.H.
Hydrocarbon Research Inc. 425

**COAL LIQUEFACTION PROCESS STREAMS CHARACTERIZATION AND
EVALUATION: AN ANALYTICAL CHARACTERIZATION CASE STUDY**

Brandes, S.D.; Robbins, G.A.; Winschel, R.A.; and Burke, F.P.
CONSOL Inc. 455

THE EFFECT OF DISPERSED CATALYSTS ON FIRST STAGE COAL LIQUEFACTION

Cugini, A.V.; Krastman, D.; Lett, R.G; and Ciocco, M.V.
Pittsburgh Energy Technology Center
Erinc, J.B.
Gilbert Commonwealth, Inc. 485

CONCEPTUAL DESIGN AND ECONOMIC EVALUATION OF BCL PROJECT

Katsushima, S.; Yoshida, T.; Kitamura, H.; and Ueda, S.
New Energy and Industrial Tech. Dev. Org. (NEDO), Japan 503

LIQUEFACTION STUDIES ON VICTORIAN BROWN COAL

Allardice, D.J.; Camier, R.J.; and Perry, G.J.
Coal Corporation of Victoria, Australia 519

LIQUEFACTION CHARACTERISTICS OF WYOMING COAL

Ikeda, K.; Endoh, K.; and Mochizuki, M.
Nippon Steel Corporation, Japan
Inokuchi, K.; Yamamoto, H.; and Yamagiwa, H.
Mitsui SRC Development Co., Ltd., Japan 537

CATALYTIC MULTI-STAGE LIQUEFACTION OF COAL

Lee, L.K.; Pradhan, V.R.; Stalzer, R.H.; and Comolli, A.G.
Hydrocarbon Research Inc. 547

CATALYTIC HYDROTHERMAL PRETREATMENT AND HYDROGENATIVE PRETREATMENT FOR ENHANCED COAL LIQUEFACTION OVER DISPERSED MoS_2

Song, C.; Schobert, H.H.; Hatcher, P.G.; Saini, A.K.; and Huang, L.
The Pennsylvania State University 561

THE EFFECTS OF DIFFERENT DRYING PROCESSES ON COAL LIQUEFACTION YIELDS

Miknis, F.P.; Turner, T.F.; and Netzel, D.A.
Western Research Institute 591

MITIGATING CROSSLINKING REACTIONS THROUGH PRECONVERSION STRATEGIES

McMillen, D.F.; Malhotra, R.; and Manion, J.A.
SRI International 605

SURFACTANT STUDIES FOR BENCH SCALE OPERATION

Sharma, P.K., and Hickey, G.S.
Jet Propulsion Laboratory, California Institute of Technology 631

NEW DIRECTION TO PRECONVERSION PROCESSING OF COAL

Nishioka, M.; Bendale, P.G.; Laird, W.; and Zeli, R.A.
Viking Systems International 647



AR - COAL LIQUEFACTION

TITLE: STEAM PRETREATMENT FOR COAL LIQUEFACTION

AUTHORS: R.A. Graff, V. Balogh-Nair, O. Ivanenko, C. Brathwaite

INSTITUTION: The City College of New York
New York, NY 10031

CONTRACT NUMBER: DE-AC22-90PC90052

PERIOD OF PERFORMANCE: 26 September 1990 to 25 January 1994

ABSTRACT

Steam pretreatment, the reaction of coal with steam at temperatures well below those usually used for solubilization, was investigated both through the aquathermolysis of model compounds and in laboratory scale tests of direct liquefaction.

Two ethers having the structure $Ar'-CH_2-O-Ar$ were synthesized and purified: α -naphthylmethyl phenyl ether (NPE) and α -benzyl naphthyl ether (BNE). After pretreatment, about half of the starting material was found to be isomeric starting material for both α -BNE and α -NPE rather than decomposition product. This isomerization was inhibited to a considerable extent using zeolite to reduce molecular mobility.

Only small differences in conversion and product distribution are observed when steam is exchanged for inert gas. Consequently, attention has been shifted to the compounds 1-phenoxy naphthalene and 9-phenoxy phenanthrene which have been reported to be cleaved by water at 350 C though unreactive in an inert medium. This has been confirmed for the latter compound.

A rapid heating liquefaction apparatus was constructed and tests were carried out with Illinois No. 6 coal slurried in tetralin. Coal was pretreated by exposing it to 750 psia steam for 15 min. Pretreatment was verified by pyridine extraction at room temperature. Liquefaction tests were conducted with both raw and pretreated coal, under slow and rapid heating conditions, with and without exposure to air.

In rapid heating liquefaction, steam pretreatment increased the total yield, the oil yield, and decreased the yield of preasphaltenes. Yields are further enhanced by the addition of zeolites. These improvements are not observed (yields may be even lower than for raw coal) when the coal slurry is heated slowly during liquefaction or when the pretreated coal is exposed to air before liquefaction.

INTRODUCTION

Development of commercially viable and environmentally sound processes for coal liquefaction remains a formidable challenge. This work is directed at means for increasing yield, improving quality, and/or reducing the required severity in slurry liquefaction processes. Two approaches have been taken here, the pretreatment of coal with steam, and the use of zeolites in pretreatment or liquefaction. These methods have been tested on the laboratory scale and explored using model compounds.

Steam pretreatment is the reaction of coal with steam at temperatures well below those usually used for solubilization. This pretreatment has been shown to be effective in coal pyrolysis. For steam pyrolysis, it has more than doubled the liquid yield, reduced the mean molecular weight of pyrolysis liquid by 31%, and increased yields in mild extraction (Graff and Brandes, 1987; Graff et al., 1988). Studies of pretreated Illinois No. 6 coal indicate that steam reacts with the ether linkages in coal, replacing them with hydroxyl groups (Brandes, et al., 1989). The result is a partially depolymerized coal. The oxygen content of this pretreated coal is 27% that of the feed. These results suggest that steam pretreatment prior to solubilization will be beneficial to the coal liquefaction process.

Investigation of reactions of model compounds chosen to mimic the structural features in coals, under conditions similar to those encountered in liquefaction, are an important approach to understanding process chemistry. The vast majority of such work has focused on the free radical hypothesis of coal reactivity (Poutsma, 1987 and 1990). More recently, however, an extensive series of studies with model compounds has been published in which aqueous thermochemistry was explored. Studies were conducted with compounds containing a plethora of diverse functionalities (Siskin and Katritzky, 1991), including sulfur compounds (Katritzky et al., 1991; Katritzky, Balasubramanian, and Siskin, 1992) and six-membered heterocycles with one nitrogen atom (Katritzky, Lapucha, and Siskin, 1992) which showed that water-assisted chemistry using acid/base catalysis and proceeding via ionic pathways can also play a key role in breaking down the coal network. Of particular interest is the report on aquathermolysis of 1-phenoxy-naphthalene and 9-phenoxyphenanthrene (Siskin, Katritzky, and Balasubramanian, 1991). While unreactive at 350 C in inert medium, both of these diaryl ethers undergo cleavage at this temperature in water without the aid of catalyst.

We report here the effect of steam treatment on the cleavage of ether linkages in model compounds α -naphthylmethyl phenyl ether (NPE), α -benzyl-naphthylether (BNE), and 9-phenoxyphenanthrene. Thermolysis was also carried out under inert atmosphere for comparison. Since the reactor wall may affect conversions through catalysis, tests were carried out in both stainless steel and pyrex lined vessels.

Direct liquefaction of steam pretreated coals was tested in a stirred autoclave and the results compared with those from the liquefaction of raw coal.

Mechanistic considerations prompted us to initiate a novel approach to liquefaction by employing zeolites in conjunction with steam. Zeolites have well defined crystal structure and combine acid catalysis with shape selectivity. Hence, they may function in coal depolymerization in a manner similar to enzyme catalysis. Unlike

catalytic clays, such as montmorillonites, which lowered aquathermolysis conversions of model compounds and which had no significant effect on liquefaction yields from Blind Canyon coal in the absence of a metal catalyst (Artok et al., 1993), zeolites employed in conjunction with steam effected cleavage of model compounds with high efficiency. Moreover, zeolites improved liquefaction yields from steam pretreated Illinois No. 6 coal.

MODEL COMPOUND STUDIES

Pretreatment

For pretreatment (aquathermolysis) of model compounds, some type of non-flow system is needed to avoid loss of starting material or its volatile products. In order to verify the nonflow method, it was first tested with coal using extraction yield as the indicator of pretreatment. Tests of a nonflow system, comprised of an 11 to 15 ml stainless steel tube loaded with coal and water and sealed with compression fittings, gave unsatisfactory results.

To overcome these difficulties, the system was changed to nonflow, open operation. In this arrangement, the reactor outlet valve is kept closed but the reactor is continuously supplied with steam at 750 psia (described below for continuous operation). This procedure gave satisfactory results. In a pretreatment test at 350 C and 750 psia, an extraction yield of 25.0% (maf raw coal, volatiles not included) which agrees with the results obtained in continuous flow operation.

Preparation of the model compounds

Four ethers having the structure Ar'-CH₂-O-Ar were synthesized: α - and β -Naphthyl methyl phenyl ethers (α - and β -NPE) were prepared according to established procedures (Maslak and Guthrie, 1986). The ¹H nmr spectra agreed with those reported in the literature. However, hplc analysis of both compounds indicated a purity of 95% and 97% respectively. β -NPE could be obtained in a purity of >99.96% by repeated recrystallizations/triturations in pentane/ether mixtures. This procedure, however, failed to produce purities greater than 95% when applied to α -NPE. Attempted purification of α -NPE by flash column chromatography on Si gel eluted with hexane/ether led to >30% decomposition products via acid catalyzed rearrangement. Purification was effected by trituration of the crude product in ethanol, to remove unreacted α -chloromethylnaphthalene, followed by recrystallization from hexane/ether/ethanol (5/2/2) at -70°C and by repeated flash column chromatographic purification on basic alumina (instead of Si gel) to afford α -NPE in >99.5% purity. The α - and β -benzylnaphthyl ethers (α - and β -BNE) were synthesized using a modification of the procedure of Maslak and Guthrie (1986) and were purified by recrystallizations. Bisaryl ethers, 1-phenoxyphenanthrene and 9-phenoxyphenanthrene were synthesized and purified according to the procedures of Afzali et al., (1983). All products were fully characterized by ¹H and ¹³C nmr and mass spectral data.

Analysis of the condensable products from thermolysis experiments

Nuclear magnetic resonance (nmr) spectra were recorded on Bruker 200 or 300MHz instruments in CDCl₃ as solvent and are reported in δ scale relative to TMS.

High performance liquid chromatographic (hplc) analyses were carried out on a Hewlett-Packard 1090 chromatograph with a diode array uv/vis detector using a μ -Porasil column 4.5 x 250mm, eluting with hexane/ether (99/1) at a flow rate of 1 ml/min. Gas chromatography-chemical ionization mass spectral analyses (GC-CIMS) were conducted on a Finnigan SSQ-70 instrument using ammonia as reagent gas. Preparative GC experiments were carried out on a Hewlett-Packard 5890 gas chromatograph equipped with a thermal conductivity detector.

The condensable products from the pyrolysis experiments were extracted from the reactor using 4 x 3 ml portions of CH_2Cl_2 /0.1 gram of sample pyrolyzed. The methylene chloride was then evaporated to dryness under a stream of nitrogen to establish recovery yields that ranged between 70-98%. The material obtained was analyzed by GC-CIMS using a 30 m length SPB-5 fused silica capillary column (Supelco). The ^1H nmr spectrum and GC-CIMS of the mixture was also determined for reference to verify that no decomposition occurs during subsequent separation steps. Separation of the product mixture from the pyrolysis of α -NPE by preparative thin layer chromatography on alumina led to several decomposition products (detected by comparison of GC-CIMS traces and ^1H nmr with those from the original CH_2Cl_2 extract). Therefore the mixture was separated by preparative GC on a porous polymeric column Tenax-GC (Alltech) employing a linear temperature gradient program (20 degree/min). All peaks from the GC runs were collected, and the pure compounds obtained were submitted to ^1H and ^{13}C nmr as well as CIMS analyses. Pure α -NPE and β -NPE were also used to detect unreacted starting materials by coinjection. Spectroscopic data of the products obtained were identical with those reported in the literature. The structure of the copious amounts of isomerized starting materials with longer GC retention times, obtained in the pyrolysis experiments of the model compounds under inert atmosphere without steam and without addition of zeolite, were established from their ^1H nmr (in CDCl_3) and CIMS(NH_3) spectral data. Thus, rearranged starting materials, (obtained from α -NPE), *o*-naphthylmethyl phenol had peaks at δ 7.6-7.8(m), 7.1-7.5(m), 7.14(m), 6.89(t, 7.4Hz), 6.79(d, 7.4 Hz), 4.66(s), 4.14(s), and *p*-naphthylmethyl phenol had peaks at δ 7.58-7.8(m), 7.2-7.5(m), 7.07(d, 8.1 Hz), 6.74(d, 8.1 Hz), 4.54(s), 4.05(s). The rearranged starting materials, (obtained from α -BNE), *o*-benzyl-1-naphthol, had peaks at δ 8.06(m), 7.76(m), 7.43(m), 7.22-7.31(m), 5.1(s), 4.15(s), and *p*-benzyl-1-naphthol had peaks at δ 8.27(m), 7.98(m), 7.56-7.23(m), 7.17(d, 7.6 Hz), 6.82(d, 7.7 Hz), 5.18(s), 4.42(s). CIMS peaks for *o/p*-naphthylmethyl phenol and *o/p*-benzyl-1-naphthol at m/z 252 ($\text{M}+\text{NH}_4$)⁺, 235 ($\text{M}+\text{H}$)⁺.

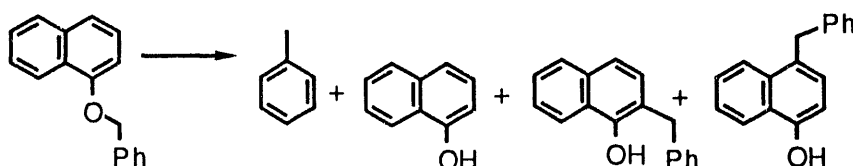
Reactions of the model compounds

In the arylmethyl aryl ether series, most testing was carried out with the α -compounds. Pretreatments were carried out in stainless steel reactors both with and without Pyrex liners. About half of the product consisted of isomeric starting material for α -BNE as well as for α -NPE, resulting from recombination of the benzyl radicals formed by homolysis, both under pretreatment conditions and under an inert atmosphere (Table 1 and 2).

α -NPE, afforded less of the isomeric starting material and more of the cleavage products when pretreatment was in stainless steel reactor without pyrex liner, possibly indicating a slight catalytic effect of the metal surface (Table 2). However, the significant difference in product distribution reported by Chawla et al. (1990), for thermolysis of α -NPE in reactors with and without glass lining was not observed.

Strategies are needed to control the reaction pathways to inhibit recombination of the initially formed primary radical species that leads to the formation of the isomeric starting materials, and hence the corresponding retrogressive type of reactions in coal, which in turn would lead to the reduced yields in lower molecular weight liquefaction products. Therefore, we attempted to reduce the mobility of the primary radical species believed to be responsible for the undesired isomerization, by carrying out the reactions in the presence of a zeolite. Table 3 shows that both under an inert atmosphere and under pretreatment conditions the zeolite accomplished this purpose: Using a stainless steel reactor, in the presence of the zeolite only 8% of isomerization product formed under inert atmosphere and none of it under steam pretreatment conditions.

Table 1. Product distributions in inert atmosphere and in pretreatment conditions for α -BNE.



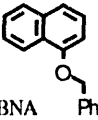
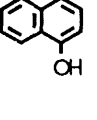
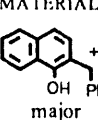
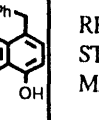
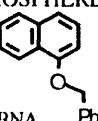
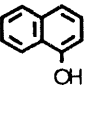
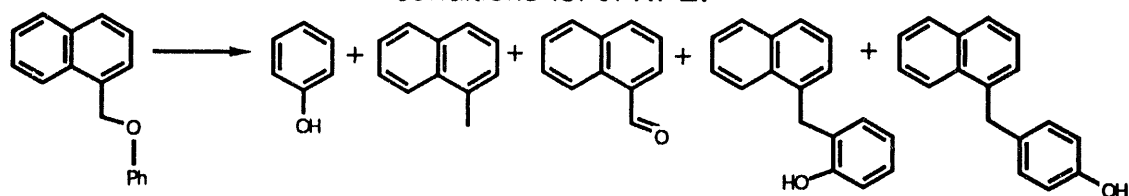
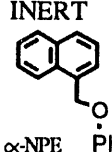


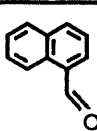
STEAM			ISOMERIC STARTING MATERIAL	RECOVERED STARTING MATERIAL	MINOR PRODUCTS
 α -BNA					
METAL	41 %	53 %	0 %	6 %	
GLASS	37 %	58 %	0 %	5 %	
INERT ATMOSPHERE			ISOMERIC STARTING MATERIAL	RECOVERED STARTING MATERIAL	MINOR PRODUCTS
 α -BNA					
METAL	42 %	49 %	0 %	11 %	
GLASS	40 %	52 %	0 %	8 %	

Table 2. Product distributions in inert atmosphere and in pretreatment conditions for α -NPE.



 α -NPE	INERT				
				recovered starting material	isomeric starting material
METAL	22.4 %	25.4 %	9.2 %	-----	43 %
GLASS	24.2 %	16.5 %	7.3 %	-----	52 %

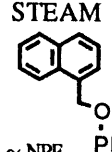

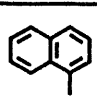
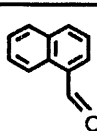
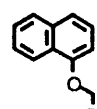
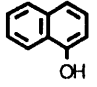
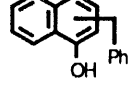
 α -NPE	STEAM				
				recovered starting material	isomeric starting material
METAL	23.1 %	22.5 %	4.3 %	9 %	41.2 %
GLASS	6.3 %	17.1 %	6 %	14.2 %	56.4 %

Table 3. Product distributions in inert and steam atmospheres for α -NPE in the presence and absence of zeolite.

	 INERT ATMOSPHERE STEAM		 INERT ATMOSPHERE STEAM	
	no zeolites	42 %	41 %	49 %
zeolites	76 %	92 %	8 %	0 %

Except in the presence of zeolite, only small differences in conversion and product distribution were observed when steam was exchanged for inert gas. Consequently, attention was shifted to the compounds 1-phenoxynaphthalene and 9-phenoxyphenanthrene because it has been reported (Siskin, et al., 1991 and 1993) that, while unreactive at 315 and 350 C in inert medium, both undergo cleavage at these temperatures in water.

The steam pretreatment of 9-phenoxyphenanthrene was carried out at the conditions used for coal pretreatment (320 C, 750 psia, 15 min). The product was almost entirely starting material.

The aquathermolysis procedure of Siskin et al. (1993) was then duplicated. One gram of 9-phenoxyphenanthrene was placed in an 11 ml 316SS reaction bomb, 7 ml of water was added, and the vessel sealed under inert atmosphere. The reactor was submerged in a fluid bath at 310 C for 1 hour. At this reaction temperature a liquid water phase is maintained and pressure reaches 1545 psia.

An analysis of the products showed no unreacted starting material. GC analysis (Tenax GC column, Alltech), and comparisons to authentic samples of phenol and phenanthrol, confirmed these to be the only two products. This duplicates the results of Siskin et al., (1993) except that they report 7.4% unreacted material and 1.2% phenanthrene.

In contrast to these results, our previous tests of this model compound at 750 psia and 15 minutes gave no observable cleavage products, only isomerized starting material. It will now be of interest to determine which of the reaction conditions are required to give high conversion.

LIQUEFACTION OF STEAM PRETREATED COAL

EXPERIMENTAL METHODS

Coal

All experiments described here were carried out with Illinois No. 6 coal from the Pennsylvania State University Sample Bank (DECS 2). The samples, received in sealed foil containers, had a particle size of -20 mesh and were determined to have a moisture content of 8.0 %. Unopened samples were refrigerated. Samples for pretreatment and liquefaction tests were ground to pass 200 mesh using an inert gas impact pulverizer. Ground coal was riffled, placed in containers, flushed with inert gas, sealed and refrigerated until used.

Pretreatment

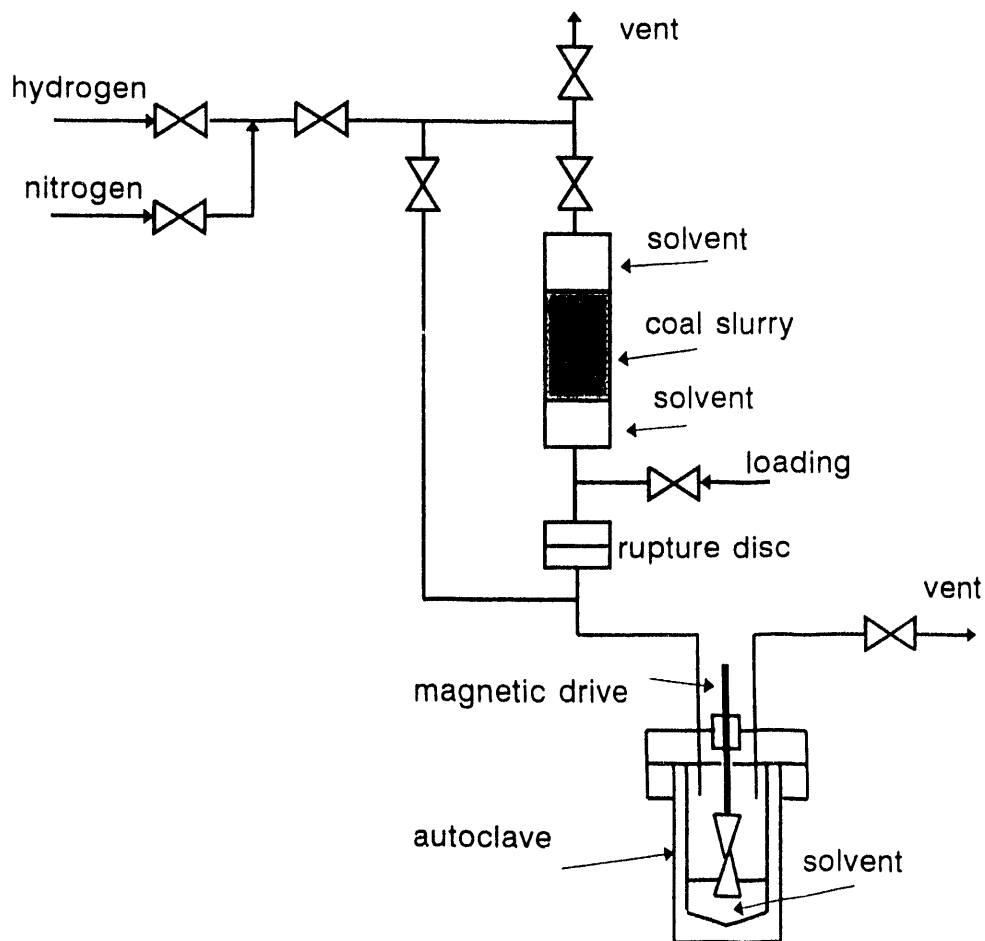
About thirty grams of coal are pretreated in each batch. The pretreatment apparatus and procedure are as described in Graff, Zhou, and Brandes (1988). After pretreatment, the reactor is opened, the contents removed, ground and sieved to pass 200 mesh. About 1.5 grams are taken for pyridine extraction. The remainder is slurried with tetralin and loaded into a glass syringe for transfer to the reservoir of the autoclave system. All of these operations are carried out in a glove box flushed with nitrogen, the gas being monitored for oxygen using a mass spectrometer. In addition, deoxygenated tetralin is used except where noted.

Liquefaction

A rapid heating liquefaction apparatus was constructed using a 300 ml stirred autoclave made of Hastelloy C and equipped with a packless magnetic stirrer drive. This was

modified by the addition of coal slurry injection line in parallel with the gas inlet line (Figure 1). The coal slurry injection line contains a stainless steel reservoir holding the coal slurry. This reservoir is separated from the autoclave by a 1000 psia rupture disc following the design of Klein and Provine, (1990).

Figure 1. Stirred Autoclave with Coal Slurry Injection.



With this apparatus the liquefaction procedure is as follows: Sixty grams of solvent (tetralin) is placed into the autoclave, and the vessel is sealed. After leak testing the autoclave with nitrogen, the reactor is flushed with hydrogen and then heated using an electric furnace. As the desired operating temperature is approached, the injection vessel is sequentially loaded with 15 g solvent, 40 g coal slurry containing 25 wt% of coal (except run 6 where 50 wt% slurry was used), and 5 g solvent using glass syringes.

When the reaction temperature (400 C) has been reached, coal slurry injection is executed by closing the gas bypass line and applying hydrogen at reaction pressure (1500 psia) to the slurry reservoir. This causes the rupture disc to burst, sweeping the coal slurry into the reactor and pressurizing the autoclave.

The injection of slurry causes an initial temperature drop, the severity and duration of which depends on whether or not the coal has been pretreated (this is discussed

below). After temperature recovery, the reactor at 400 ± 5 C for the remainder of the run. The run time is 30 minutes measured from coal injection. To terminate the run, the heater is turned off and removed from the autoclave. When ambient temperature is reached, the reactor is vented and opened. The contents of the reaction vessel are transferred to a weighed cellulose Soxhlet thimble (double thickness) using 200 ml of hexane as the transfer solvent. After the liquid is drained off at ambient temperature, the residue is extracted sequentially with hexane, toluene and THF. The thimble and its contents are dried to constant weight after 18 hours of extraction with each solvent.

From these weights, liquid yields are calculated. In addition, the weight of coal remaining in the injection system is also determined. This is subtracted from the amount of coal initially loaded into the syringe in order to calculate the weight of coal injected. From a knowledge of the weight of volatiles lost during pretreatment, the corresponding weight of daf raw coal can be calculated. Yields are reported on a daf raw coal basis. The product distribution is classified as follows: oils and gases (hexane soluble), asphaltenes (toluene soluble), preasphaltenes (THF soluble). According to Joseph (1991), the gas yield from raw Illinois No. 6 coal in slow heating liquefaction is less than 5%.

RESULTS

Twelve runs have been carried out. These are grouped in Table 4 to facilitate comparison, Liquefaction yields are given based on raw daf coal. The yield from room temperature extraction with pyridine of pretreated coal is also given as a check on the pretreatment step.

The first pair of runs (C2 and 10) are for slow heating. For the slow heating liquefaction of raw coal, the slurry is charged directly into the cold autoclave. The autoclave is then sealed, charged with hydrogen and heated. The time required to reach 400 C is 35 minutes. After 30 minutes at this temperature, the heater is removed and the autoclave allowed to cool to room temperature.

For slow heating liquefaction of pretreated coal, to prevent exposure of the pretreated coal to air, slurry is prepared and loaded into a syringe under inert atmosphere in the same way as for rapid heating liquefaction. The slurry is then injected into the autoclave also using the same procedure as in rapid heating, the difference in this case being that the reactor is at room temperature. After slurry injection, the reaction is heated to 400 C, also requiring 35 minutes. The reactor is pressurized with hydrogen to 1500 psia and maintained at this pressure and temperature for 30 minutes. The shut down and analytical procedures were then the same as for rapid heating experiments.

Steam pretreatment is detrimental in slow heating liquefaction, resulting in a lower total yield as well as lower yield in each fraction.

The second pair of runs (2 and 8) are for raw coal with rapid heating. The runs were identical; the results show the spread of the data. Rapid heating causes an increase in oil yield and decrease in preasphaltene yield. The total yield is not significantly affected.

Table 4

Liquefaction of Illinois No. 6 Coal

Run No.	Comments	Total	Conversion (wt %)			Pyridine Extraction Yield (wt %)
			Oils	Asph.	Preasph.	
C2	raw coal slow heating	81.6	37.0	16.9	27.7	18.3
10	steam treated coal, slow heating	73.8	35.2	14.4	24.2	35.1
2	raw coal rapid heating	73.8	42.2	10.0	21.6	---
8	raw coal rapid heating	80.0	48.7	16.7	14.6	20.3
6	steam treated coal, rapid heating	85.7	60.1	17.2	8.4	22.3
12	steam treated coal, rapid heating	79.3	55.8	14.7	8.8	34.7
7	steam treated coal, rapid heating	91.6	56.0	14.2	21.7	35.2
9	steam treated coal, rapid heating	85.2	47.5	17.3	20.4	38.9
11	steam treated coal, rapid heating exposed to air	66.3	38.6	19.8	7.9	32.4
13	steam treated coal, zeolite mixture, rapid heating	95.5	51.2	25.9	19.3	40.1
14	steam treated coal, zeolite mixture, rapid heating	96.2	53.5	17.3	25.4	33.0
15	steam treated coal, zeolite mixture, rapid heating	98.1	63.8	18.8	15.5	35.0

These two runs are the basis for comparison with steam treated coal liquified under rapid heating conditions.

The next four runs (6, 12, 7 and 9) are for steam pretreated coal liquified under rapid heating. Runs 6 and 12 were made with deoxygenated tetralin. These runs show a definite increase in oil yield and decrease in preasphaltene yield.

Run 7 and 9 were made with tetralin from bottles which had been previously opened and not protected against oxygen absorption. The principal effect of this absorbed oxygen in the solvent appears to be a pronounced increase in preasphaltene yield.

The importance of preventing pretreated coal from being exposed to oxygen is demonstrated by run 11. In this run, the pretreated coal was deliberately exposed to air for an hour before slurrying with deoxygenated tetralin. In all other respects the procedure followed was the same as that for liquefaction of pretreated coal. The most important result is a pronounced decrease in oil yield, even below the value for raw coal with rapid heating. The total yield is also decreased. Asphaltenes are higher than the anaerobic case while preasphaltenes are lower.

A potentially significant difference in temperature history following injection of coal into the autoclave is observed according to whether raw or pretreated coal is used. For example, in run no. 12, using pretreated coal, the temperature drop was 41C. In run C2, coal slurry injection resulted in a temperature drop of 88 C. A similarly large temperature drop (60 C) was observed in a simulated rapid liquefaction test in which solvent without coal was injected. The absence of such a large temperature drop is significant because it indicates the occurrence of exothermic reactions in pretreated coal exposed to hydrogenation conditions which do not occur in raw coal. It will be of interest to identify these reactions.

The highest total conversion yields (95.5-98.1%) were obtained in runs 13-15 where an equal amount of a zeolite was added to the coal sample during the steam pretreatment stage. This added zeolite was not removed, but carried over into the liquefaction stage. Although consistently high yields of oils (51-63.8%) were obtained in the presence of the zeolite, these were comparable, but not higher than the yields obtained without zeolite in case of steam treated coal, under rapid heating conditions. Since the yields of asphaltenes and preasphaltenes were somewhat higher, and extraction with pyridine gave consistently high yields, this suggests that the zeolite helps to break-down the 3D network of the coal during the steam pretreatment stage. Further experiments are necessary to verify this by adding the zeolite after the steam pretreatment stage.

It is interesting to speculate how the zeolite brings about the increase in total liquefaction yields observed in runs 13-15. Zeolites, or aluminosilicates, are microporous solids with channels and interconnecting cavities forming pores in their crystal structures (Catlow, 1992). They are used in more than 90% of the catalytic cracking units in the United States, in which the heavier components of crude oil are converted to smaller molecular weight compounds (Newsam, 1993). Zeolites are highly versatile materials since their acid-base and catalytic properties can be modulated by synthesis by adjusting the Si/Al ratio, and by varying the nature of the attached cations. The 5A zeolite we employed in runs 13-15, Table 4, has the molecular formula

$\text{Ca}_{4.5}\text{Na}_3[(\text{AlO}_2)_{12}]\cdot 30\text{H}_2\text{O}$ and has a nominal pore diameter of nearly 5\AA . Since it does not contain Si atoms, it is a zeolite of low acidity. Although the results are preliminary, and we need to employ zeolites of diverse acidity and pore/supercage properties, it can be hypothesized that during steam pretreatment of coal, aquathermolysis type reactions that follow ionic pathways are important. Another major role the zeolite may play is restricting the mobility of structural fragments of the coal, thus anchoring it at "active sites" enabling the formation of low energy transition states where the orientation of the reactants is optimized.

CONCLUSIONS

Steam pretreatment has beneficial effect on slurry liquefaction provided that the pretreated coal is protected from exposure to oxygen and that it is rapidly heated during liquefaction. The most pronounced effect, under conditions studied here, is to improve the product quality by increasing oil yield while decreasing preasphaltene yield.

The observed temperature history following coal slurry injection indicates exothermic hydrogenation reactions occurring in pretreated coal which are absent in raw coal.

Zeolites enhance the effect of steam in the thermolysis of arylmethyl aryl ethers by completely inhibiting retrogressive reactions. The same mechanism may be responsible for the high conversion yields obtained when zeolites are added to coal in the steam pretreatment-liquefaction tests.

PLANS

Model Compound Studies

It is potentially of considerable interest for understanding steam pretreatment that:

- A. None of the model compounds so far studied by us, arylmethyl aryl ethers, at conditions used for coal treatment, show any substantial effect when the atmosphere is switched from inert gas to steam.
- B. That all of the ethers studied by Siskin, et al. (they did not test arylmethyl aryl ethers), only 1-phenoxy-naphthalene and 9-phenoxyphenanthrene were cleaved in water but not in inert medium.

We have so far reproduced the results of Siskin, et al. with 9-phenoxyphenanthrene. We will now proceed to determine what conditions are necessary for the cleavage of this model compound by conducting tests at intermediate conditions. These tests will include tests with 1-phenoxy-naphthalene and tests at new conditions with some of the arylmethyl aryl ethers and 4-(1-naphthylmethyl)bibenzyl (compound I). Some tests will also be made using zeolites together with the model compound to alter product distribution.

Liquefaction tests

Additional Tests with Illinois No. 6 Coal

Liquefaction tests of Illinois No. 6 coal have so far been carried out only at our standard conditions of 400 C and 30 min. Additional tests will be carried out at lower (350 C, 20 min) and higher severity (450 C, 60 min) to assess the effect of steam pretreatment on product distribution at these conditions. This will help guide the selection of conditions for process development and may help us to understand pretreatment.

Tests with Other Zeolites

Since the results with 5A zeolite look promising, tests will be made with other zeolites having both distinctly larger and smaller pores. The acidity of zeolites is strongly affected by the Si/Al ratios and the nature of the zeolites' cation(s), therefore a few selected zeolites with differing acidity will also be tested. Some exploration of time and temperature effects will also be made.

Tests so far have been made with zeolite present in both pretreatment and liquefaction. It will be especially important to establish the role of zeolite in each step separately. This will be done by conducting a test series with zeolite present in one step but not the other.

Tests with Other Coals

So far only Illinois No 6 coal is known to give improved liquefaction yields as a result of pretreatment. At least two additional coals will be selected for liquefaction tests. These tests are needed to demonstrate that Illinois No. 6 is not unique and that the method is applicable to other coals. Results with othr coals will also provide information which will help us to understand pretreatment chemistry.

Analysis of Liquefaction Products

In addition to gas analyses, the analysis of liquefaction products will be expanded to include boiling point distribution, elemental analyses, molecular weight determination, and gas chromatography of lighter constituents.

Pretreatment Tests

Two analyses are of interest in order to better understand steam pretreatment chemistry. Analysis of pretreatment volatiles will be carried out using the procedure now being developed for liquefaction gas. The major components of the pyridine extract from pretreated coal will be characterized by such methods as HPLC, MS, FTIR, NMR and elemental analysis.

REFERENCES

- Afzali, A., H. Firouzabadi and A. Khalafi-Nejad (1983) Synth. Commun., **13**, 335.
- Artok, L., P.B. Malla, S. Komarneni and H.H. Shobert (1993), Energy and Fuels, **7**, 430.
- Brandes, S.D., R.A. Graff, M.L. Gorbaty, and M. Siskin (1989), Energy and Fuels, **3**, 494.

Catlow, C.R.A. In "Modeling of Structure and Reactivity in Zeolites," C.R.A. Catlow, Ed., Academic Press, 1992, pp. 1-18.

Chawla, B., B.H. Davis, B. Shi, and R.D. Guthrie (1990), Preprints ACS Division of Fuel Chemistry, **35**, No. 2, 387.

Graff, R.A. and S.D. Brandes (1987), Energy and Fuels, **1**, 84.

Graff, R.A., P. Zhou and S.D. Brandes (1988), "Steam Conditioning of Coal for Synfuels Production," Final Report for 1987 to 1988, U.S. Department of Energy, Contract No. DE-AC21-87MC23288.

Joseph, J.T. (1991), Fuel, **70**, 139.

Katritzky, A.R., A.R. Lapucha, and M. Siskin (1992) Energy and Fuels, **6**, 439.

Katritzky, A.R., M. Balasubramanian, and M. Siskin (1992) Energy and Fuels, **6**, 431.

Katritzky, A.R., M. Murugan, M. Balasubramanian, J.V. Greenhill, M. Siskin, and G. Brons (1991) Energy and Fuels, **5**, 823.

Klein, M. and W. Provine (1990), private communication.

Newsam, J.M. (1986) Science, **231**, 1094.

Maslak, P. and R.D. Guthrie (1986), J. Am. Chem. Soc., **108**, 2637.

Poutsma, M.L. (1987) A Review of Thermolysis Studies of Model Compounds Relevant to the Processing of Coal, Report ORNL/TM-10637

Poutsma, M.L. (1990) Energy and Fuels, **4**, 113.

Siskin, M. and A.R. Katritzky (1991) Science, **254**, 231 and references therein.

Siskin, M., A.R. Katritzky, and M. Balasubramanian, (1991) Energy and Fuels, **5**, 770.

Siskin, M., A.R. Katritzky, and M. Balasubramanian (1993) "Aqueous Organic Chemistry. 5. Diaryl Ethers: Diphenyl Ether, 1-Phenoxynaphthalene and 9-Phenoxyphenanthrene," accepted for publication, Fuel.

THE DUAL ROLE OF OXYGEN FUNCTIONS IN COAL PRETREATMENT AND LIQUEFACTION: CROSSLINKING AND CLEAVAGE REACTIONS[†]

Michael A. Serio, Erik Kroo, Sylvie Charpenay, Rosemary Bassilakis, Peter R. Solomon, Donald F. McMillen*, Apparao Satyam*, Jeffrey Manion*, Ripudaman Malhotra*

Advanced Fuel Research, Inc., East Hartford, CT

*SRI International, Menlo Park, CA

[†]Work supported under Contract No. DE-AC22-91-PC91026

INTRODUCTION

It has become increasingly clear in recent years not only that retrograde reactions substantially hinder the liquefaction of low-rank coals, but also that oxygen functional groups in the coal structure are major actors in these retrograde reactions. The evidence connecting oxygen groups to the formation of new, strong bonds, though convincing, is largely phenomenological in nature rather than mechanistic. Thus we know that crosslinking is correlated with the evolution of CO₂ and H₂O and therefore that carboxyl and/or phenolic groups are involved, but we do not know exactly how or why. In order to best mitigate the retrograde reactions, it is necessary to better understand their mechanisms i.e., to know what factors promote and inhibit these reactions. It is also known that oxygen groups, such as phenols, can promote bond scission reactions, so it can be difficult at the present time to predict the net impact of a new pretreatment. The overall objective of this project is to elucidate and model the dual role of oxygen functions in thermal pretreatment and liquefaction of low rank coals through the application of analytical techniques and theoretical models. The project is an integrated study of model polymers representative of coal structures, raw coals of primarily low rank, and selectively modified coals in order to provide specific information relevant to the reaction of real coals.

Studies were done on samples of Argonne Zap Lignite and Wyodak subbituminous coals which have been demineralized and exchanged with calcium, barium or potassium cations. In most cases, two sets of modified coal samples were prepared: 1) vacuum-dried; 2) exposed to water vapor until an equilibrium moisture content was reached. The samples were characterized by FT-IR transmission analysis in KBr pellets, programmed pyrolysis in a TG-FTIR system and liquefaction in donor solvent. Three variations of the linear polymer [-C₆H₃(R)CH₂CH₂-O]_n, where R=H, OMe, and OH were prepared and characterized. The thermal behavior of these polymers was studied by pyrolysis-FI mass spectrometry (Py-FIMS) and TG-FTIR. The decarboxylation and coupling behavior of a series of a series of monomeric aromatic and aliphatic carboxylic acid structures under homogeneous, but liquefaction-relevant reaction conditions was also studied.

EXPERIMENTAL

Coal Demineralization and Modification Apparatus

A literature review of various demineralization methods was completed. Experimental techniques found in the literature for coal demineralization (1) and ion-exchange (2,3) use batch type reactors to carry out the given treatment of coal, which necessitates filtering of the coal sample any time the solvent is changed. Based on this review, an apparatus for continuous-flow, controlled-atmosphere demineralization and controlled pH ion-exchange of coals and other related materials was designed and constructed. The different solvents are held in separate reservoirs which are all equipped with sparge valve systems to deoxygenate the solvents before use (with N₂ or He as needed).

Preparation of Demineralized and Ion-Exchanged Coal Samples

Demineralization. - The procedure was similar to that described in the work of Bishop and Ward (1). The coal samples used in this study were the Zap and Wyodak coals from the Argonne premium sample

bank (4). The samples were all -100 mesh. Before starting the acid treatment, the samples were thoroughly wetted by mixing with de-ionized water under a nitrogen environment. Demineralization involved washing the coal with a flow of 2M HCl for 45 minutes, 50% HF for 45 minutes, 2M HCl for 45 minutes, and de-ionized water for 120 minutes. The process was performed at 80 °C.

Ion-Exchange of Carboxyl Groups with Cations - The acidity constant (k_a) of carboxylic acids is around 10^{-5} , and that of phenols is around 10^{-10} . Theoretically, almost all carboxyl OH can be exchanged with cations at pH 8, whereas the phenolic-OH can remain in the acid form, according to the following equation:

$$\frac{[A^-]}{[HA]} = \frac{k_a}{[H^+]} \quad (1)$$

where HA is either the carboxyl or phenolic group in the acid form. At pH 8, $[A^-]/[HA]$ would be a value of order 10^3 for carboxyl groups, and 10^{-2} for phenols. Schafer's experimental results also suggest that the carboxyl groups in coal can be completely exchanged with cations at a pH around 8-8.5 (2). 1N barium acetate solution, which has a pH value around 8.2, was used for ion-exchange of carboxyl groups with barium. Roughly 3 g of demineralized coal was mixed with 300 ml of 1N barium acetate in a cell under a nitrogen environment. After 5 minutes of mixing, the pH value of the mixture dropped to less than 7.5. The mixture was filtered through a Teflon membrane by increasing the nitrogen pressure, and the mixing cell was refilled with another 300 ml of barium acetate. The pH value of the solution dropped again after mixing. The filtration and refilling procedure was repeated, usually 15-20 times, until the pH value of the mixture in the cell reached 8.0 ± 0.1 and remained constant with mixing. The drop of the pH value was probably due to the release of H^+ from carboxylic acids in the coal.

The mixture was kept under continuous mixing conditions in a nitrogen environment for at least 20 hours before the acetate solution was purged out, and the cell was refilled with a final 300 ml charge of 1N barium acetate. After 10 minutes of mixing, the acetate solution was purged out, and the coal sample was washed with 150-200 ml of de-ionized water. The coal sample was then removed from the cell for vacuum drying, which lasted for at least 20 hours. The sample was kept in a nitrogen box after drying. A similar procedure was used for exchanging calcium and potassium cations, starting with the metal acetate.

Ion-Exchange of Phenolic and Carboxyl Groups with Cations - According to equation 1, both phenolic and carboxyl groups can be totally exchanged with cations at pH around 12.5. Schafer (2) reported that the exchange of -OH groups was complete at pH 12.6. In this study, a solution, recommended by Schafer, of 0.8 N $BaCl_2$ and 0.2 N $Ba(OH)_2$ having a pH of 12.7, was used for ion-exchange with barium cations.

Approximately 3 g of a demineralized coal sample was stirred with 300 ml of the pH 12.7 solution in a nitrogen environment. After 5 minutes of mixing, the mixture was filtered through a membrane and the cell was refilled with another 300 ml of the pH 12.7 solution. The purging and refilling procedure was repeated 3 times, and the pH value of the final mixture was around 12.6. The mixture was continuously mixed under a nitrogen environment for at least 20 hours for exchange. After this long-time exchange period, the solution was purged out, and the cell was refilled with the pH 12.7 solution. After 10 minutes of mixing, the solution was purged out, and the coal sample was washed with a solution of 0.1 N $BaCl_2$ and 0.03 N NaOH, which has a pH around 12.7, to avoid hydrolysis of the exchanged coal. The coal sample was then removed from the cell for vacuum drying. After drying, the sample was kept in a nitrogen box for further study. A similar procedure was used for exchanging calcium and potassium cations.

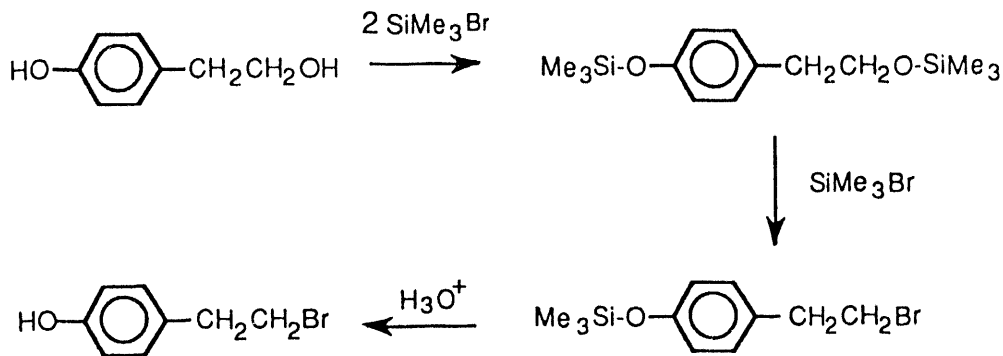
Preparation of Moisturized Coal Samples

A procedure for restoring the moisture level of modified coal samples was developed. The moisturized samples were prepared by enclosing the vac-dry modified samples in a box with a nitrogen purge of

100% humidity. The sample exposure to moisture was performed for several days (~6 days) until no further moisture uptake was observed.

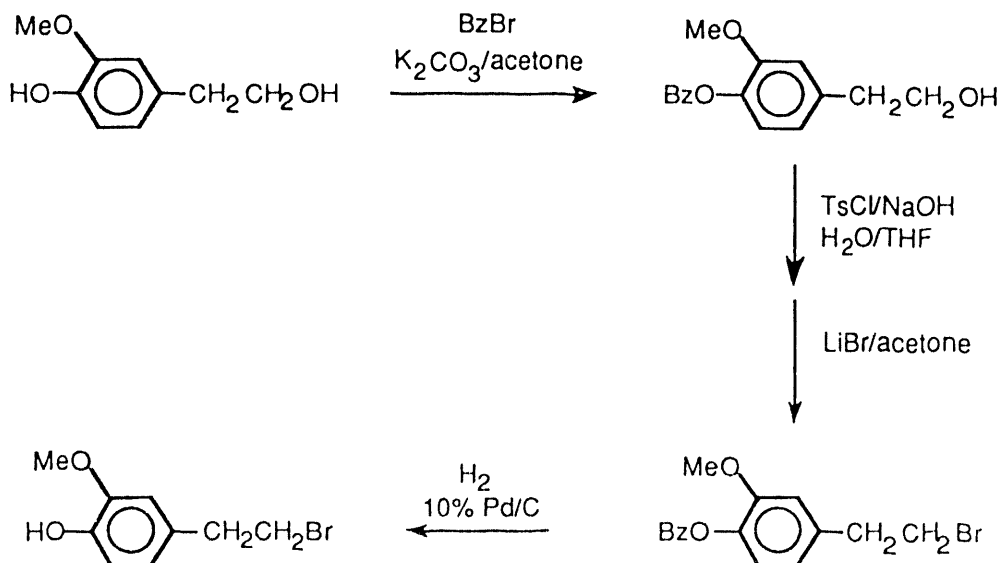
Preparation of Model Polymers

Synthesis of $-\text{[C}_6\text{H}_3(\text{o-OR})\text{-CH}_2\text{CH}_2\text{O}]_n-$ Polymers. - The polymer with R = H was synthesized by basic phase-transfer catalysis polymerization of 4-hydroxyphenethyl bromide using tetrabutyl-ammonium hydroxide as the basic catalyst. The 4-hydroxyphenethyl bromide was obtained in turn via a three-step synthesis involving the silylation of both oxygens of 4-hydroxyphenethyl alcohol, followed by nucleophilic displacement of the siloxy group from the aliphatic carbon and hydrolysis of the nucleophile-resistant siloxy group directly attached to the aromatic ring. This sequence is outlined in Scheme 1.



Scheme 1. Synthetic route to the $-\text{[C}_6\text{H}_3(\text{H})\text{CH}_2\text{CH}_2\text{O}]_n-$ polymer.

The -C-C-O- polymer with R = OMe was synthesized by similar phase-transfer base catalyzed polymerization of 4-hydroxy(3-methoxy)phenethyl bromide. This material was obtained by subjecting 4-hydroxy(3-methoxy)phenethyl alcohol (homovanillyl alcohol) to a sequence of displacement reactions that required, because of the presence now of two phenolic groups (-OH and -OMe), a more complex protection scenario to ensure that only the desired -OH groups were derivatized at the desired time. The sequence utilized is shown in Scheme 2.



Scheme 2. Synthetic route to the $-\text{[C}_6\text{H}_3(\text{o-OCH}_3)_c\text{H}_2\text{C}_H\text{2}_d]_n-$ polymer.

At various intermediate stages, the products were isolated and characterized by solution-phase NMR to insure adequate purity. The chemical shifts allow one to readily distinguish between $-\text{CH}_2\text{OH}$, $-\text{CH}_2\text{OTs}$, $-\text{CH}_2\text{Br}$, and $-\text{CH}_2\text{-OPh-}$ at 3.85, 4.3, 3.4, and 4.15 ppm relative to TMS, respectively. Adequate purity was particularly important for the 4-hydroxy(3-methoxy)phenethyl bromide polymer precursor, since purification after polymerization is impractical. For this reason, the 4-hydroxy(3-methoxy)phenethyl bromide product of the catalytic hydrogenolysis in Step 4 was purified by column chromatography. For all those intermediates that were soluble in CHCl_3 or THF, solution-phase ^{13}C - and ^1H - NMR showed the intermediates to be of the correct structure and to have total impurity levels less than 5%. GPC of the THF-soluble portions of the polymers indicated weight average molecular weights ranging from about 2000 to 4000. Therefore all polymers had average $n > 15$.

In order to compare the effects of $-\text{OMe}$ groups and free $-\text{OH}$ on depolymerization and crosslinking and thereby to gain additional insight into the impact of methylation of phenolic $-\text{OH}$ in low-rank coals, it was desirable to convert some or all of the methoxy groups in the $-\text{[C}_6\text{H}_3(\text{o-OMe})\text{OCH}_2\text{CH}_2\text{]}_n-$ polymer to $-\text{OH}$. Partial demethylation of the ortho-methoxy substituted polymer was achieved by treatment with trimethylsilyl iodide and lithium iodide, which was found to work better in this case than various versions of the methods of Harrison (5) or McKervey and co-workers (6). NMR analysis of the partially demethylated material showed that less than one $\text{CH}_2\text{-O}$ linkage was cleaved for every twenty ArO-CH_3 bonds that were cleaved, so that there was little molecular weight reduction that by itself would affect volatile yields.

RESULTS AND DISCUSSION

The modified coal samples were characterized by FT-IR transmission analysis in KBr pellets, programmed pyrolysis in a TG-FTIR system and liquefaction in donor solvent. The model polymers were characterized by GPC, NMR, FT-IR and pyrolysis - FIMS. The model compounds were reacted in micro-autoclaves under liquefaction related conditions. The results are discussed below.

Experiments with Modified Coal Samples

Effect of Cations on Pyrolysis Tar and Liquefaction Yields - The results of sample analysis by programmed pyrolysis in the TG-FTIR are shown in Figs. 1 and 2, and summarized in Table 1 for the Zap lignite. These results show that demineralization tends to increase the tar yield, whereas both the gas and char yields were reduced. Similar results were observed for the Wyodak coal (7,8). Table 1 also shows a decrease of the tar yield with the extent of ion-exchange with the metal cations, and a corresponding increase in the total amount of gas evolution. The liquefaction results for different samples are shown in Table 2. The data in Tables 1 and 2 show that the yields of both the pyrolysis tar and toluene solubles from liquefaction decrease with the extent of ion-exchange, i.e., in the order of (demineralized) $>$ (ion-exchanged at pH 8) $>$ (ion-exchanged at pH 12.5). This result indicates that having the carboxyl or phenolic groups in the salt form makes it easier to crosslink the coal structure during pyrolysis or liquefaction reactions.

It is realized that this is a more difficult comparison for the samples exchanged at pH 12.5, since considerable amounts of humic acids were observed to dissolve in the high pH value solutions. The dissolution of coals in the aqueous alkaline solutions may be due to the breaking of ester bonds in coal, i.e., $\text{RCOOR}' + \text{OH}^- \rightarrow \text{RCOO}^- + \text{R}'\text{OH}$. This coal dissolution mechanism was also proposed by other workers (9). The solubility of coal in alkaline solutions varies with the cations contained in the solution. The color difference of the calcium and potassium solutions after ion-exchange at high pH is striking, in that the potassium solution has a much darker color, indicating much more coal dissolved in the monovalent cation (K^+ here) solution than the bivalent cation (Ca^{++} here) solution. The results also show that the barium solution extracted more coal than the calcium solution, but not as much as the potassium solution. A possible reason is the fact that Ca^{++} and Ba^{++} ions can act as cross-links between two acid groups of different coal fragments (9), whereas K^+ can only interact with one acidic site. The ability of bivalent cations to act as initial crosslinks in the structure at high pH is supported by data on the pyridine volumetric swelling ratios (VSR) and pyridine extractables, shown in Table 3. The values of the VSR are lower for the bivalent cations at high pH for both the dry and moist coals. It can be seen in Table 1, for the pyrolysis of vacuum dried samples, that the tar yield was higher for the potassium-exchanged coals than the calcium and barium-exchanged samples at high pH, suggesting that bivalent

Table 1. Pyrolysis Results of Vacuum Dried Modified Zap Samples.

Coal (type/preparation)	Pyrolysis Products (wt.%, daf)					
	Tars	CO ₂	CO	H ₂ O	CH ₄	Char
Fresh	7	8.9	14.7	14.3	2.2	57
Demin.	20	4.8	10.4	8.4	2.7	54
Demin. + K ⁺ (pH8)	11	8.6	9.9	16.0	1.9	57
Demin. + Ca ⁺⁺ (pH8)	10	8.6	13.5	10.3	2.4	58
Demin. + Ba ⁺⁺ (pH8)	6	11.7	15.8	18.6	2.6	55
Demin. + K ⁺ (pH12.5)	5	9.9	12.4	13.5	1.6	57
Demin. + Ca ⁺⁺ (pH12.5)	4	8.2	22.6	12.6	2.0	51
Demin. + Ba ⁺⁺ (pH12.5)	3	10.5	24.1	15.5	2.6	52

Table 2. Liquefaction Results of Vacuum Dried Modified Zap Samples.

	Toluene Solubles			Gas		
	Total	Oils	Asphaltenes	CO ₂	CO	CH ₄
Fresh	26	12	14	4.3	0.24	0.25
Demin.	52	26	26	1.1	0.43	0.27
Demin. + K ⁺ (pH8)	30	11	19	7.7	0.27	0.17
Demin. + Ca ⁺⁺ (pH8)	25	13	12	2.7	0.30	0.22
Demin. + Ba ⁺⁺ (pH8)	37	25	12	7.3	0.40	0.20
Demin. + K ⁺ (pH12.5)	17	5	12	5.0	0.24	0.27
Demin. + Ca ⁺⁺ (pH12.5)	*	*	3	0.7	0.04	0.08
Demin. + Ba ⁺⁺ (pH12.5)	15	15	0.5	0.3	0.27	0.02

* Yields Calculated by Difference were Negative. Solvent Incorporation is Suspected.

Table 3. Characterization of Cation-Exchanged Zap Samples.

Coal Type	Dry			Moist			
	V.S.R.	P _s	Moisture	V.S.R.	P _s	Moisture	
Zap Raw	2.7	5	NM	1.9	15	32	
Zap Demin.	3.1	20	4	2.6	22	16	
pH 8	K ⁺	2.0	10	6	1.9	9	20
	Ba ²⁺	1.8	3	5	1.5	4	22
	Ca ²⁺	2.1	6	5	1.6	6	21
pH 12	K ⁺	1.7	2	6	1.4	2	29
	Ba ²⁺	1.1	2	7	1.2	2	22
	Ca ²⁺	1.1	1	9	1.2	1	25

Notes: V.S.R. = Volumetric Swelling Ratio in Pyridine; P_s = Pyridine Solubles (daf)
Moisture was Determined by TG-FTIR and is Reported on an As-received Basis.
NM = Not Measured.

Table 4. The Carbonyl and Phenolic Contents of Zap and Wyodak Coals Determined by Barium Titration. (meq g⁻¹ daf basis)

	Carboxyl Groups	Phenolic Groups	Total Acidity
Zap Lignite	2.52	6.74	9.26
Wyodak Sub.	2.40	5.76	8.16

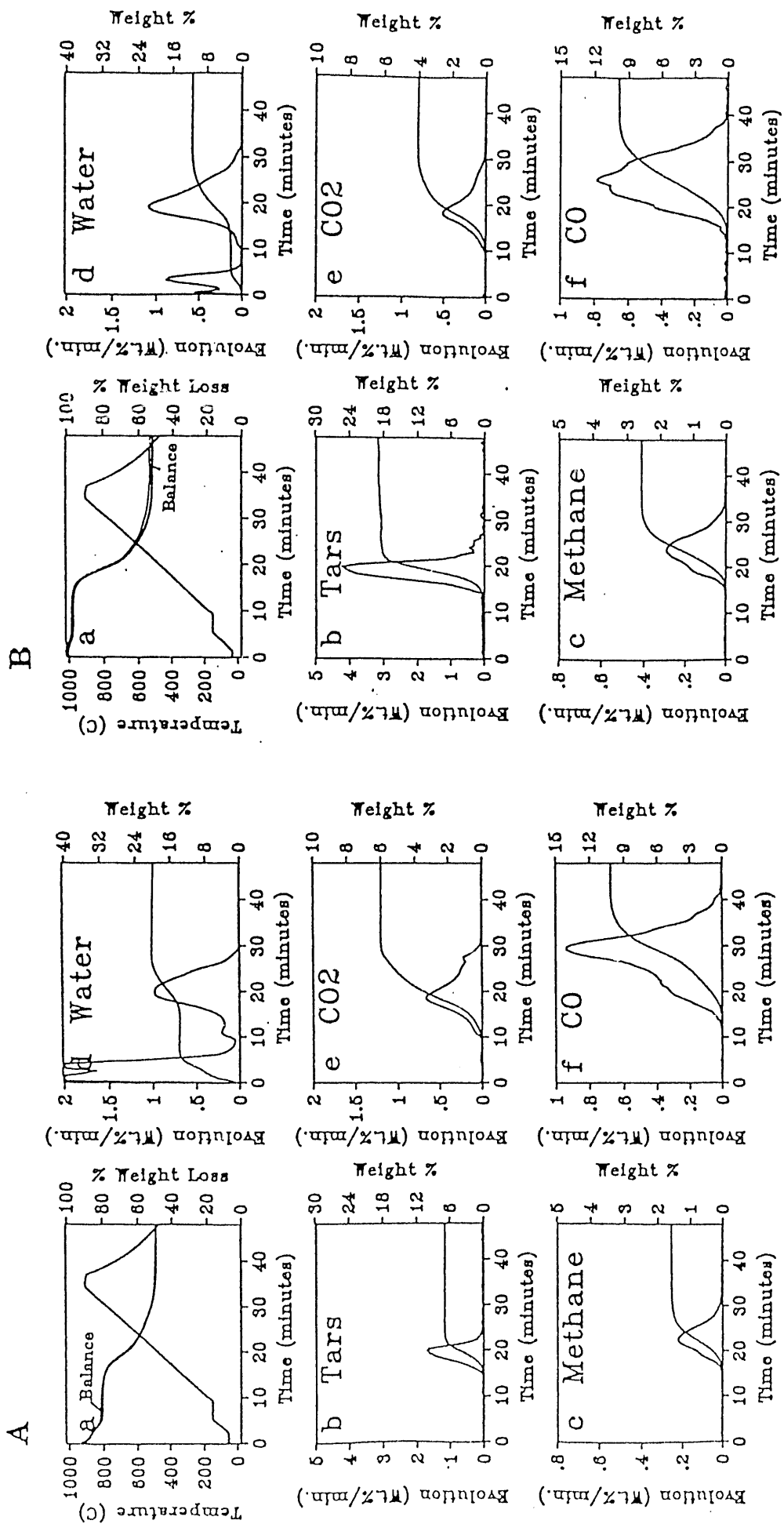


Figure 1. TG-FTIR Analysis of A) Raw and B) Demineralized Argonne Zap Lignite.

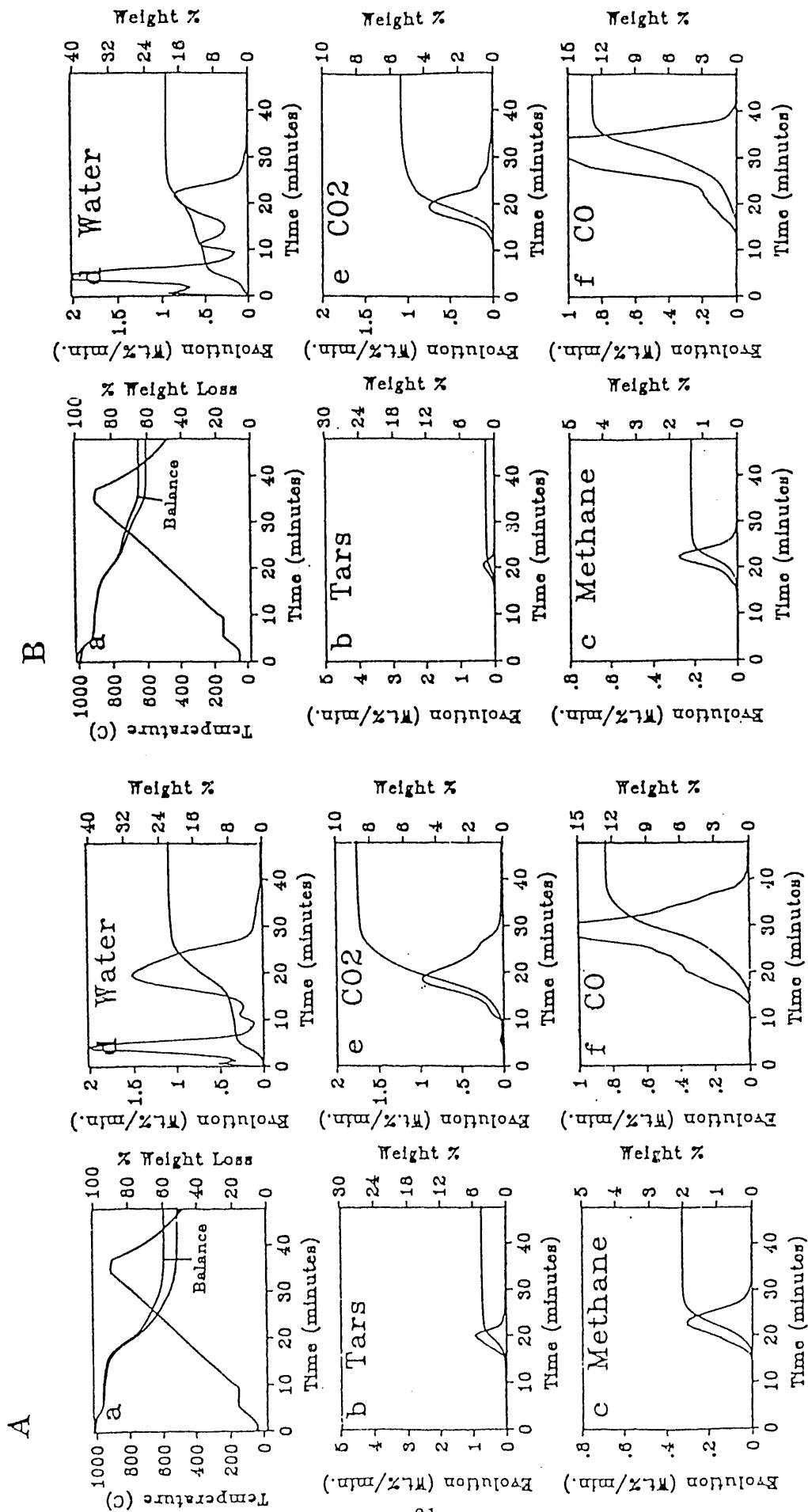


Figure 2. TG-FTIR Analysis of Zap Samples which A) have had Carboxyl Groups Exchanged with Barium; B) have had Carboxyl and Phenolic Groups Exchanged with Barium.

cations tighten the coal structure by cross-linking coal fragments and making it more difficult for tar molecules to form (10). At pH 8, the values of the tar yield and VSR for the monovalent and bivalent cations are more similar, though lower than the values for either the raw or demineralized coals. Consequently, it appears that the monovalent cations help to hold the structure together, although this must occur through electrostatic rather than covalent interactions. It makes sense that valency would be less important in the normal state of the coal or at pH=8 since, for steric reasons, cations are unlikely to be exchanged on more than one carboxyl or ortho-dihydroxy site.

Effect of Cations on Gas Yields from Pyrolysis and Liquefaction - It is of interest to note that the gas yields from liquefaction and pyrolysis do not always follow the same trend. Table 1 shows that, in pyrolysis, the total yield of oxygen-containing gases (i.e., CO₂, CO, and H₂O) always increases with decreasing tar yield. Table 2 shows the expected increase of the liquefaction yields with tar yield. However, the gas yields in liquefaction show an irregular variation with pH and with cation type. For example, the CO₂ yield is high for the partially barium exchanged Zap lignite, and is significantly reduced for the completely barium exchanged sample. The Wyodak subbituminous coal shows the opposite trend (7,8). For the ion-exchanged Zap lignite, the decrease of the CO₂ yield in liquefaction can be explained by the loss of some organic components, which contain CO₂-forming functions, during the barium exchange at high pH. Some of these variations could be due to catalysis of secondary gas-phase or gas-solid reactions.

For CO evolution in pyrolysis, the demineralized samples show the major evolution at temperatures between 400 and 800 °C, as shown in Fig. 1b for the Zap Lignite. CO evolution also occurs in a similar temperature range for fresh and ion-exchanged sample, as shown in Figs. 1a and 2. However, the evolution is depressed at temperatures lower than about 750 °C, but elevated above this temperature by comparing with that of the demineralized samples. It was also noted that the fraction of CO evolving before 750 °C increases with increasing tar yield, as shown in Fig. 3a for the Zap lignite. This observation is significant. The higher CO evolution at temperatures lower than 750 °C for demineralized samples could be due to more oxygen functions evolving as CO without crosslinking. For ion-exchanged samples, the depressed CO evolution at lower temperatures is probably caused by oxygen retention through crosslinking between oxygen functions, and the CO evolved at 750 °C or above, is likely from the decomposition of the metal carboxylate groups which can produce carbonates as a decomposition product. The raw and cation exchanged samples have a sharp evolution peak in the TG-FTIR analysis, as shown in Figs. 1a and 2. This occurs in the same temperature range as the decomposition of carbonates and could be the result of catalytic gasification of the CO₂ produced to CO. The correlation of the total CO evolution in coal pyrolysis with pyrolytic tar and liquefaction yields was studied, as shown in Fig. 3b for the Zap lignite. The data shows that both tar and liquefaction yields increase with decreasing total (pyrolysis) CO yield. Therefore, both the relative amount of CO evolved before 750 °C and the total CO evolution are indicators of the extent of crosslinking.

Figures 1 and 2 also show that CO₂, H₂O, and low temperature CO evolve in a similar temperature range. This result suggests that these products are derived from a consecutive mechanism. The CO₂ evolution curve does not show as much shape variation with changes in cation content. However, the yield is basically a decreasing function of tar yield. In previous work, the relationship between CO₂ evolution and crosslinking events has been noted (10-13). This has been explained by the mechanism that elimination of CO₂ would create aryl radicals to enhance crosslinking. The current study provides further evidence for the relationship between CO₂ evolution, retrogressive reactions and cation content. The CH₄ yield also showed a trend opposite to that of the tar yield for the ion-exchanged samples. This has been generally reported in coal pyrolysis studies (14). By reincorporation into the solid matrix by more stable bonds, the tar precursors can yield volatiles only by cracking off small side groups, hence the increased CH₄ yields with decreasing tar yields.

One aspect of the H₂O evolution data revealed in Figs. 1 and 2 merits further comment. For samples which contain acidic functions in the salt form, including fresh and barium exchanged samples, there is always a water evolution peak present at around 200 °C. This 200 °C peak is obscure for demineralized samples. It is very likely that this peak is due to the evolution of moisture which is ionically bonded on the salt structure. For vacuum dried samples, it can be seen that the moisture content increases with the cation content in the samples, as shown in Table 3. This indicates that the acidic functions in the salt forms attract polar water molecules. These attracted water molecules cannot

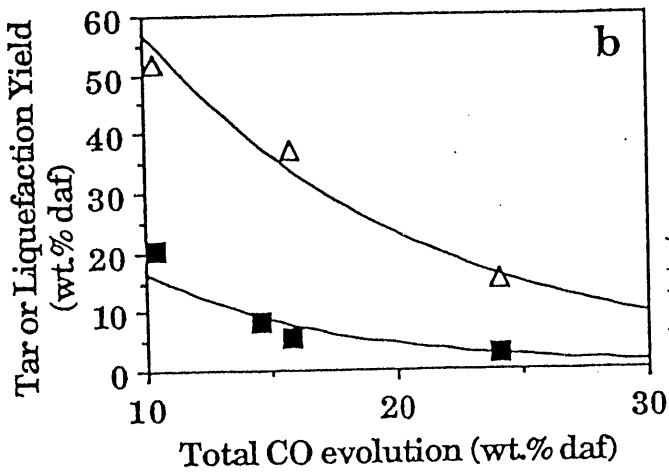
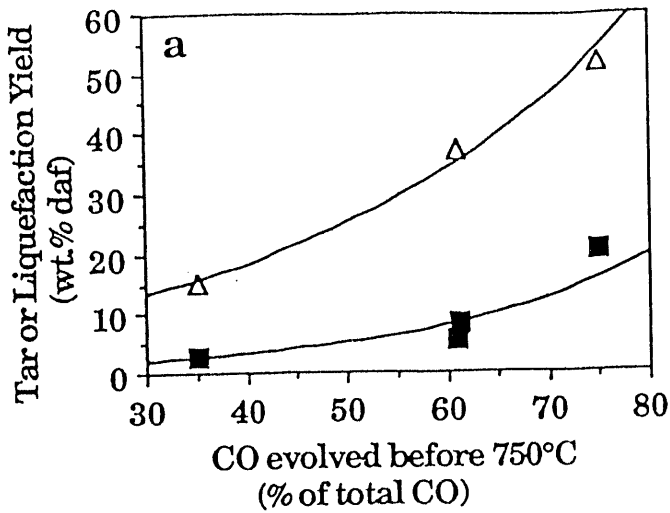


Figure 3. Correlation of Pyrolysis Tar Yield (■) and Toluene Solubles from Liquefaction (Δ) for Zap Lignite with a) Pyrolysis CO Evolution Before 750°C; b) Total Pyrolysis CO Evolution.

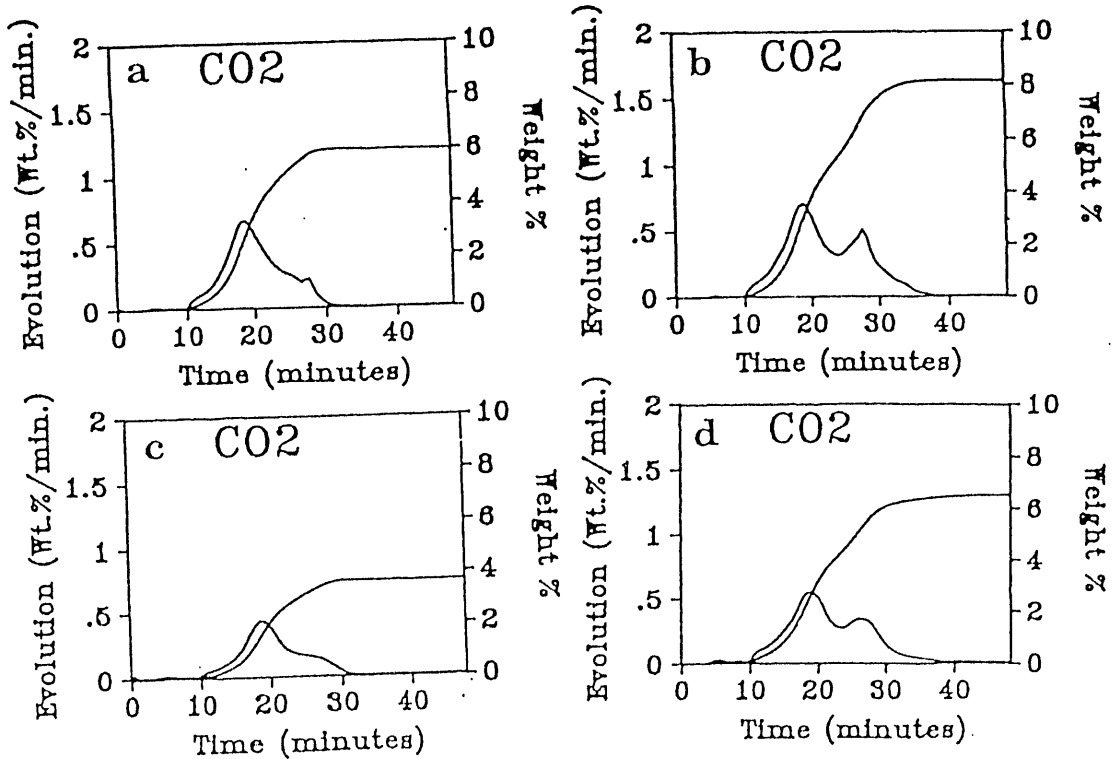


Figure 4. CO₂ Evolution During Coal Pyrolysis. a) Raw Zap; b) Remoisturized Zap; c) Raw Wyodak; d) Remoisturized Wyodak.

be removed by vacuum drying, but only by raising the temperature of the sample. The relationship between cations and moisture has important implications as far as retrogressive reactions in liquefaction system are concerned, as discussed below.

Analysis of Carboxyl and Phenolic Groups by Barium Titration - In theory, all of the carboxyl groups of demineralized samples can be exchanged with barium at pH 8. Consequently, it follows that one could determine the concentration of carboxyl groups in coal by knowing the amount of barium ion-exchanged at pH 8. The chemical composition of ash formed by combustion of the barium exchanged sample is predominantly BaO. Therefore, from the ash content of the samples ion-exchanged at pH 8, one can estimate the concentration of carboxyl groups in the coal. Similarly, the total concentration of carboxyl and phenolic groups can be determined by the ash content of the sample ion-exchanged at pH 12.6. The concentration of phenolic groups can be obtained from the difference of the above two measurements. The concentrations of carboxyl and phenolic groups determined in this manner for Zap and Wyodak are shown in Table 4. The results shown in Table 4 are similar to those determined by Schafer (2,15) for Australian low-rank coals, using barium titration methods. However, our FT-IR results indicate that not all of these groups can be exchanged and that the cations can interact with additional sites in the coal (7,16).

Pyrolysis and Liquefaction of Moisturized Coal Samples - Remoisturization of vacuum dried Zap and Wyodak was done in the attempt to understand if moisture uptake for low rank coals is a reversible process and to see if moisture influences the role of the cations. The remoisturized samples were analyzed by programmed pyrolysis with TG-FTIR. Preliminary results show that the moisture content can reach that of the raw samples by remoisturization for Zap, but not for Wyodak. The results for the Zap lignite are shown in Table 3. Furthermore, the chemical structure of the coal samples seems to have been changed by remoisturization, since different CO₂ evolution behaviors were observed. A comparison of the CO₂ evolution behavior for raw and remoisturized coal samples is given in Fig. 4. The effects of moisture on the yields of gaseous and liquid products from pyrolysis and liquefaction were relatively modest, especially in the case of pyrolysis (7,8,17). A possible explanation for the difference is that most of the moisture is depleted early in the pyrolysis process, whereas the moisture is retained in the reactor during liquefaction and can exist in a liquid phase. The detailed liquefaction and pyrolysis results are presented in Ref. 8.

It is also known from our results (See Table 3) and the literature (15) that the moisture is associated with cations in raw coals. Consequently, an investigation was made to determine if the deleterious effects of cations could be mitigated by adding water to the donor solvent liquefaction system. Results from experiments with raw and demineralized Zap at three different temperature levels are given in Table 5. At temperatures near or below the critical temperature of water (374° C), it appears that there is a profound beneficial effect of added water for the raw coal (note the significant reduction in CO₂ evolution). Conversely, there is a significant deleterious effect of added water for the demineralized coals. The ability of water to interact with cations and affect the course of the thermal decomposition behavior is consistent with results that have been observed in hydrothermal treatment of coal (18-20), which mimics the geological aging process in many respects.

Table 5. Effect of Added Water on Liquefaction of Raw and Demineralized Argonne Zap Coal.

Temp. Level (°C)	Water Addition	Toluene Solubles wt.%, daf		CO ₂ Yields wt.%, daf	
		Raw	Demin.	Raw	Demin.
350	yes	13	0	0.0	1.1
	no	1	27	5.4	2.4
375	yes	23	19	2.4	1.5
	no	11	40	5.2	2.2
400	yes	31	24	5.2	0.8
	no	30	58	4.1	4.2

Experiments with Model Polymers

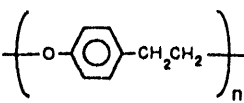
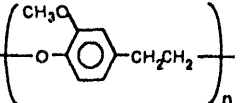
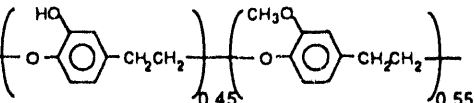
Introduction. The pyrolysis of prototypical lignin-related structures provides an opportunity to address a critical question relating to the liquefaction behavior of low-rank coals: "What makes some of these coals highly reactive, but very difficult to solubilize in the early stages of a liquefaction process?" With the objective of beginning to answer this question, we have synthesized $-\text{[C}_6\text{H}_3(\text{o-OR})\text{-CH}_2\text{CH}_2\text{O}]_n-$ polymers where R = H, OCH₃, or OH, and have performed pyrolytic decomposition studies using pyrolysis-field ionization mass spectrometry (Py-FIMS) and FTIR-detected thermogravimetric analysis (TG-FTIR).

Mechanistic studies on pyrolysis or liquefaction of coal "model compounds" have most often utilized materials that are very poor representatives of coals, either because the linkages in these models are not the probable critical linkages in coals and/or because the models are not polymeric. Thus either the required bond-cleavage reactions themselves are inappropriate and/or the structural fragments are not released into an environment that even modestly represents any of the mass-transfer limitations of real coals. In order to address these limitations, we have prepared and studied the pyrolytic behavior of a class of polymers having the structure $-\text{[C}_6\text{H}_3(\text{R})\text{CH}_2\text{CH}_2\text{-O}]_n-$. These polymers have the "β-ether" linkage that is known to be dominant in the lignin precursors of low-rank coals, and which one expects to be substantially retained in these coals, but do not have any of the aliphatic alcohol groups of the lignins themselves. The cleavage of this linkage has been previously (21-24) examined in the compound β-phenylphenethyl ether, but has not, to our knowledge, been incorporated into polymeric models for the purpose of addressing the bond cleavage and crosslinking reactions that occur during coal liquefaction or pyrolysis. Although the real coals presumably have had crosslinks generated from condensation of aliphatic alcohol groups (present in the original lignin) during coalification, understanding the behavior of the original β-ether linkages is a first and critical step to understanding how some low-rank coals can be so reactive and yet difficult to solubilize.

Pyrolysis Techniques. Both the TG-FTIR and pyrolysis-FIMS techniques used here have been previously described (25,26). TG-FTIR uses programmed-temperature pyrolysis in flowing He and provides weight-loss and volatile product information primarily for fixed gases and light hydrocarbons. FIMS employs programmed-temperature pyrolysis at high vacuum and provides molecular ion mass spectra for organic products evolved as a function of temperature.

General Pyrolysis Results. Volatiles yields were high for all three polymer variations (83-87% at one atmosphere and 80-100% under vacuum, Table 6), and the temperature of maximum volatiles generation (T_{max}) values were all similar, about 400°C at one atmosphere, and 350°C in vacuum (at heating rates of 30° and 4°C/min, respectively). The weight-loss curves are all very steep at T_{max} , with half-lives of 100 seconds or less. Figure 5 shows the TG-FTIR weight loss curve for the base polymer $-\text{[C}_6\text{H}_3(\text{H})\text{CH}_2\text{CH}_2\text{O}]_n-$. Figures 6 and 7 show the pyrolysis-FIMS curves for the polymers $-\text{[C}_6\text{H}_3(\text{R})\text{CH}_2\text{CH}_2\text{O}]_n-$ where R = H and OMe, respectively. The data for polymers having R = H, OMe, and a 45/55 mixture of OH and OMe are summarized in Table 5. Figures 5 through 7 also show for comparison expected decomposition rates based on data in the literature for phenylphenethyl ether. Depending on the temperature and which literature data are chosen, the rates observed for these polymers are 10 to 200 times faster than those reported for the basic C-C-O prototype, phenylphenethyl ether.

Table 6. Pyrolysis Data for $-\text{[C}_6\text{H}_3(\text{o-OR})\text{-CH}_2\text{CH}_2\text{O]}_n-$ Polymers

WEIGHT-LOSS DATA	POLYMER STRUCTURE		
			
TG-FTIR			
Tmax (°C), 1 atm He	427	421	421
% Wt Loss @ 900°C	87	83	86
k dec (%/min @ Tmax)	0.40	0.64	0.51
Pyrolysis-FIMS			
Tmax (°C), in vacuum	325	350	330
% Wt Loss @ 500°C	80	100	100
k dec (%/min @ Tmax)	0.4	>0.5	0.3

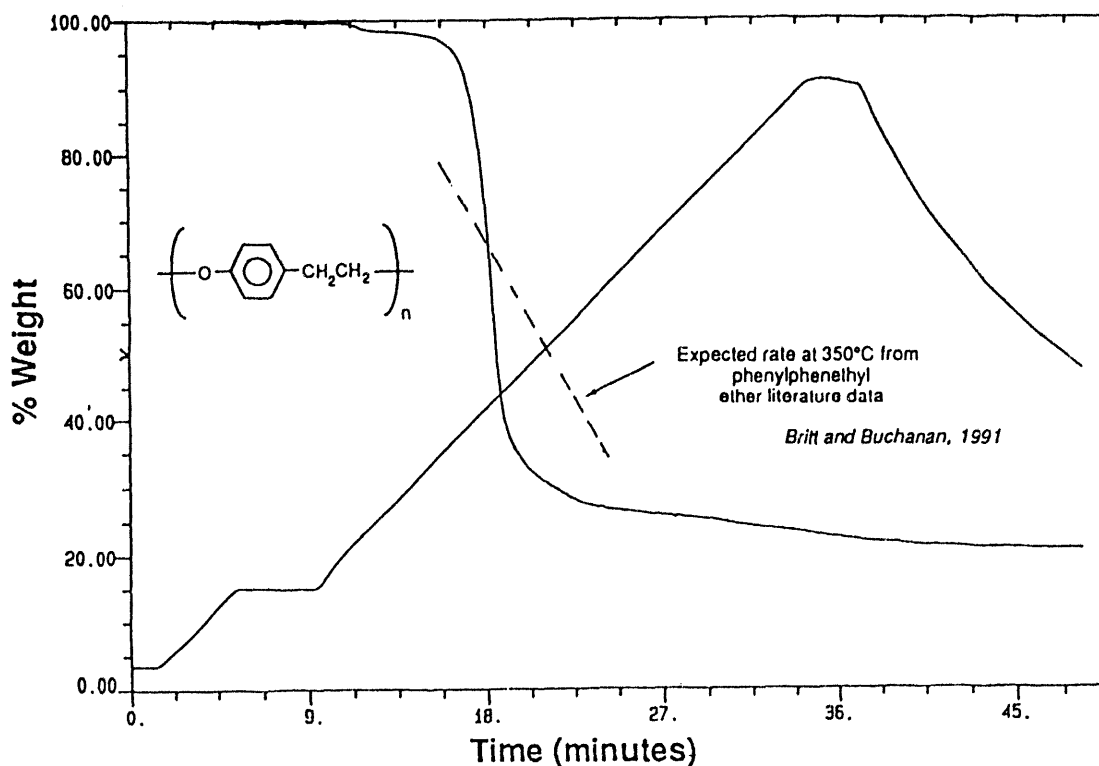


Figure 5. TGA-FTIR Weight Loss Curve for $-\text{[C}_6\text{H}_3(\text{H})\text{CH}_2\text{CH}_2\text{O]}_n-$ Polymer.

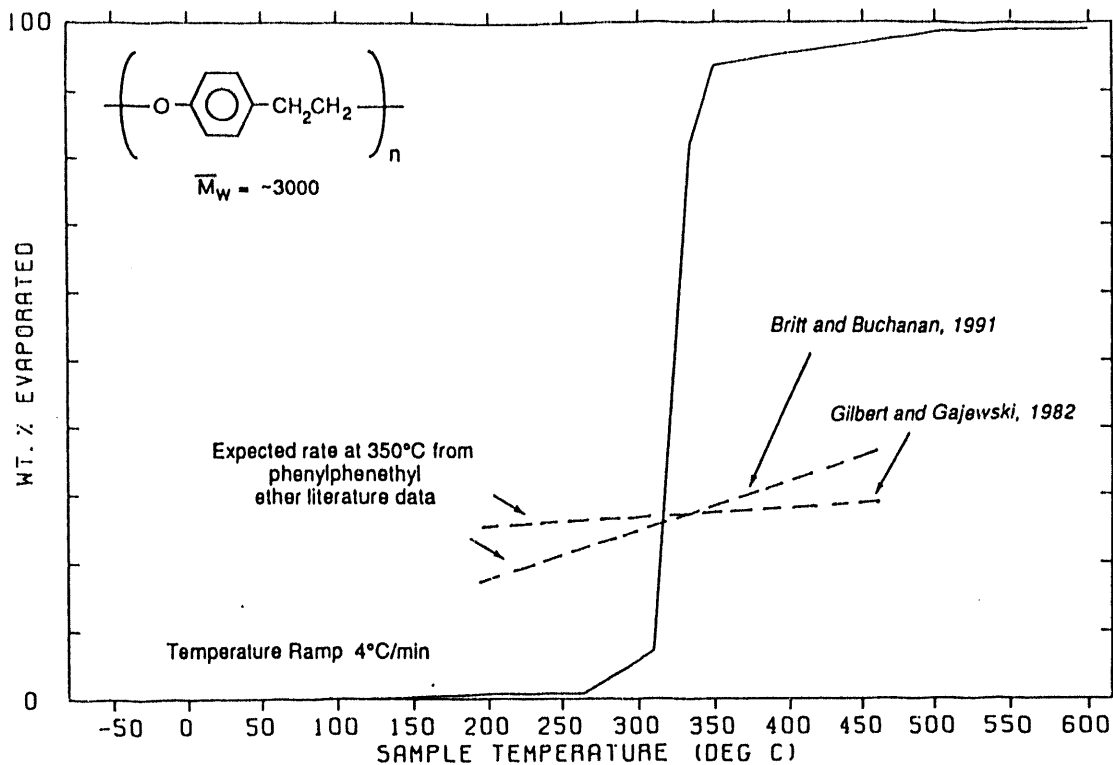


Figure 6. Pyrolysis-FIMS Vacuum Vaporization Curve for $-\text{[C}_6\text{H}_3(\text{H})\text{CH}_2\text{CH}_2\text{O}]_n-$ Polymer.

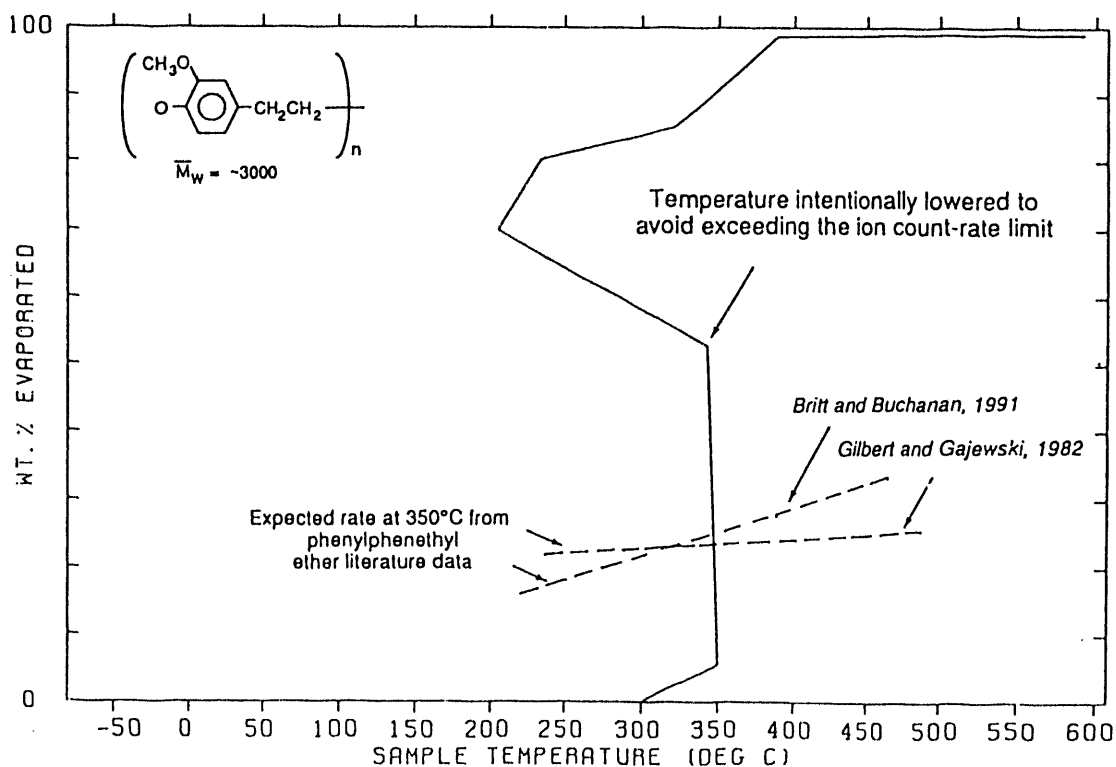
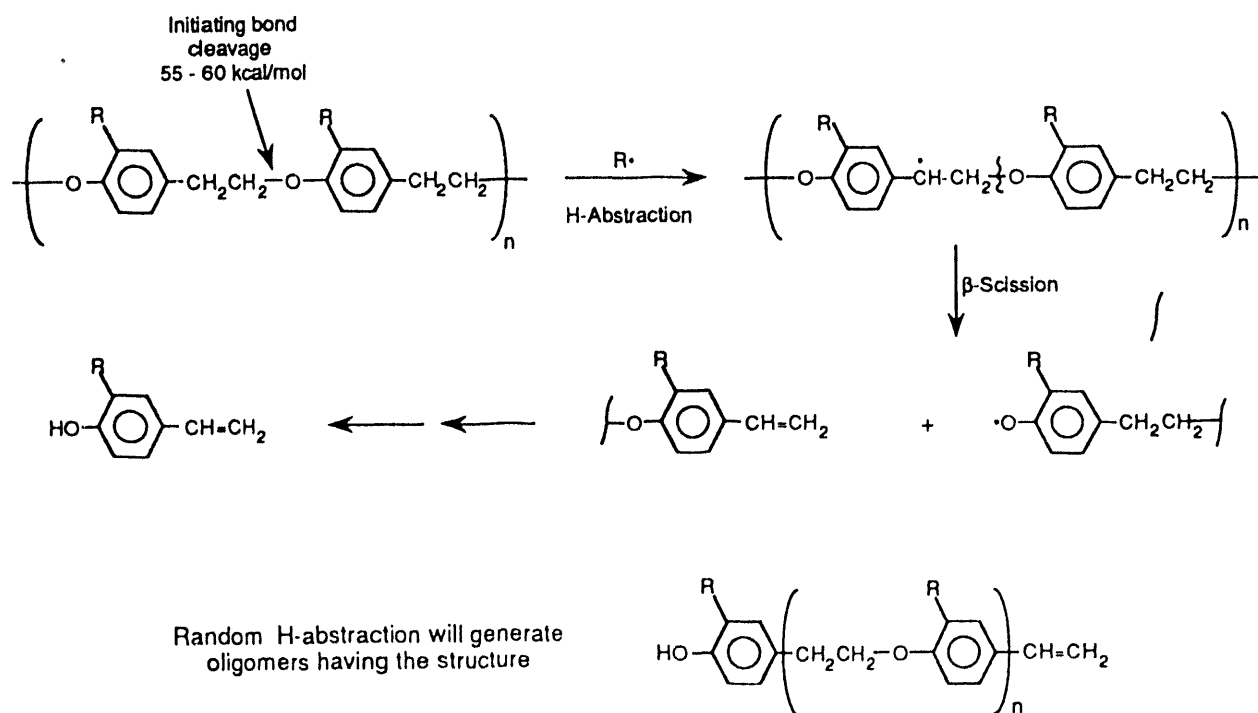


Figure 7. Pyrolysis-FIMS Vacuum Vaporization Curve for $-\text{[C}_6\text{H}_3(\text{OMe})\text{CH}_2\text{CH}_2\text{O}]_n-$ Polymer.

Oligomeric Products and Possible Depolymerization Mechanism. Figures 8 and 9 show the pyrolysis-FI mass spectra for $-\text{[C}_6\text{H}_3(\text{R})\text{CH}_2\text{CH}_2\text{O]}_n-$ where R = H and OMe, respectively. The masses and structures for many of the major peaks are noted in the figures. Spectra for all of the polymers are similar in general terms, showing a series of oligomers with a double bond in one of the C_2 groups, resulting from non-reductive cleavage of the polymer linkages. In all cases, a pronounced dominance of monomer over dimer, trimer, etc., *from the onset of decomposition through its completion* indicates that the linkages are being cleaved in a coordinated, or unzipping manner, rather than through random attack on the polymer chain. The presence of a free hydroxy group (rather than an aryl-alkyl ether linkage) on the terminal aromatic ring system somehow makes the linkage to the para position of that ring system more subject to cleavage. Lignins show a similar, and as yet unexplained, coordinated cleavage (27).

One can qualitatively rationalize this unzipping by postulating that the radical-chain H-abstraction— β -scission processes known to account for the decomposition of monomeric -C-C-O- linked structures (i.e., phenylphenethyl ether) would here lead to the chain -transfer, H-abstraction reactions occurring preferentially on the end unit. This sequence is illustrated in Scheme 3. However, there are several difficulties with a simple extension of the phenylphenethyl ether decomposition sequence. First, in view of the probable coiled configurations of these linear polymers, and thus the probable proximity of many interior chain positions, preferential H-abstraction from the end unit does not seem likely. Second, the observed rates of polymer pyrolysis are 10-200 times faster (in TG-FTIR and Py-FIMS, respectively) than is rationalizable by assuming that the bond strength differences (see Table 7) are applied to the net reaction rate according to the simple expression for the rate of propagation of a chain process having a second-order chain breaking step [rate of reaction $\propto r_p(r/r_b)^{1/2}$]. Third, the methoxy-substituted polymer exhibits a more pronounced autocatalytic behavior than the basic (i.e., H-substituted) polymer.



Scheme 3. Possible radical-chain unzipping sequence for -O-C-C- polymers.

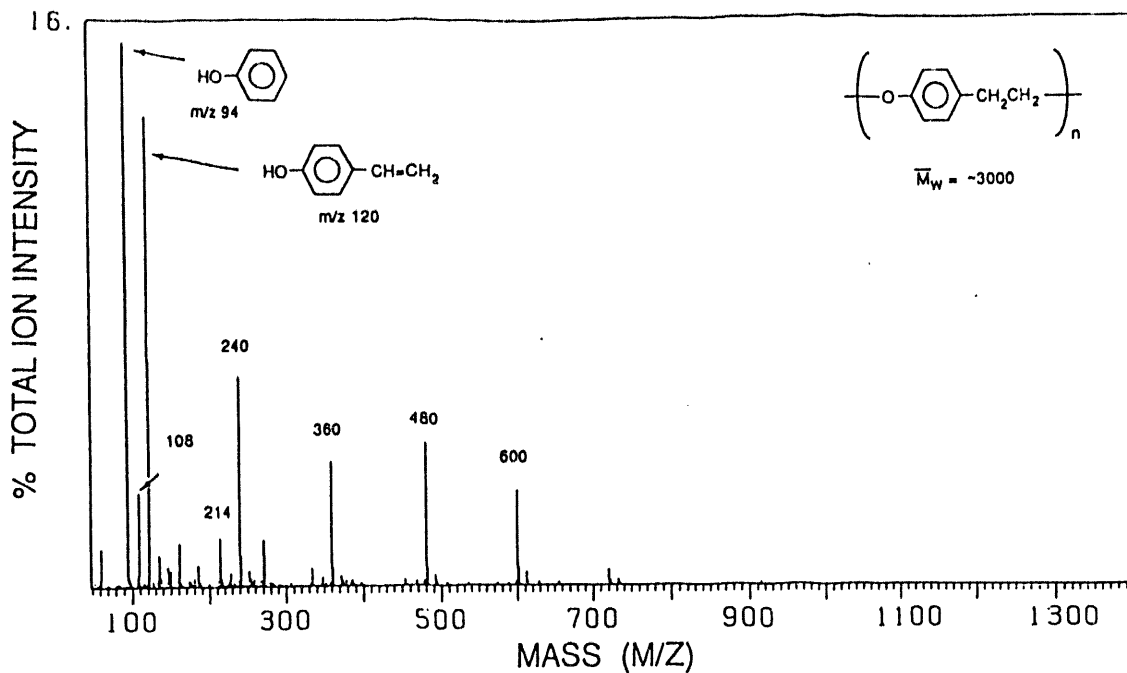


Figure 8. Pyrolysis-FI Mass Spectrum of $-\text{[C}_6\text{H}_3(\text{H})\text{CH}_2\text{CH}_2\text{O}]_n-$ Polymer.

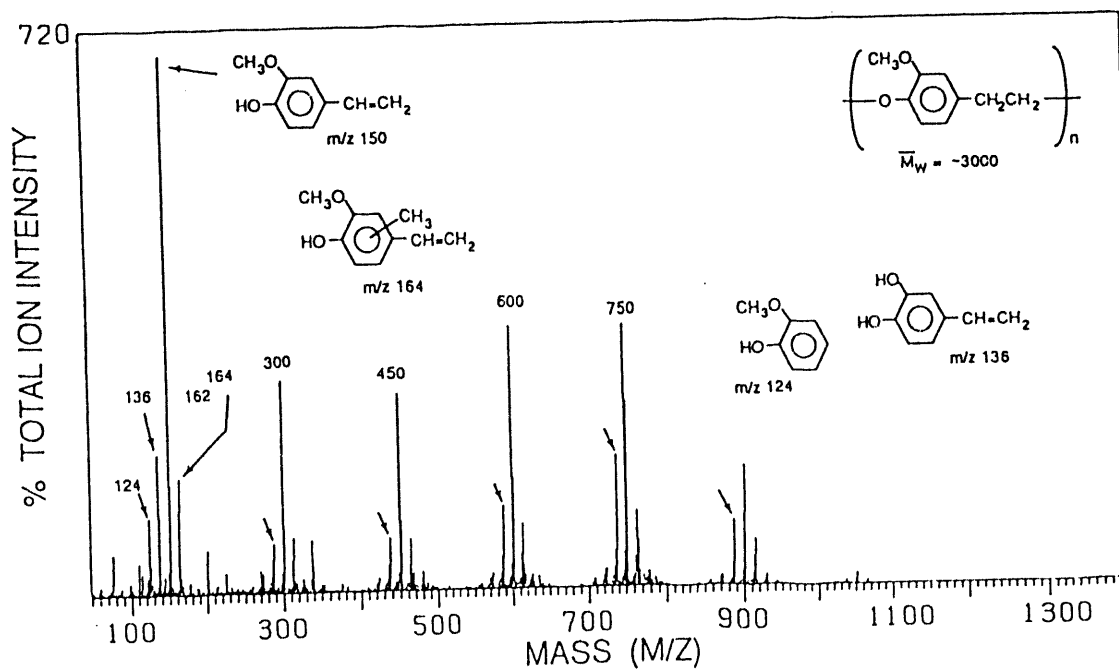


Figure 9. Pyrolysis-FI Mass Spectrum of $-\text{[C}_6\text{H}_3(\text{OCH}_3)\text{CH}_2\text{CH}_2\text{O}]_n-$ Polymer.

Table 7. Thermochemistry^a and Expected and Observed Rates of β -Ether Polymer Pyrolysis

Structure	$\Delta H^\circ(\text{Init})$	$\Delta H^\circ(\text{abst})$ (kcal/mol)	$\Delta H^\circ(\beta\text{-scission})$	Relative Rates pred.	Relative Rates obs.	Obs. Half-life (min, @350°C)
	61	-1.5	12	1	1	400 ^b
	59	0	11	2	200	2
	55	+4	9	1-5	>250	<2
	52	+6	6	0.3	150	3

TABLE 7 FOOTNOTES

a. Bond strength data and estimates of bond strengths are taken from References 28-30

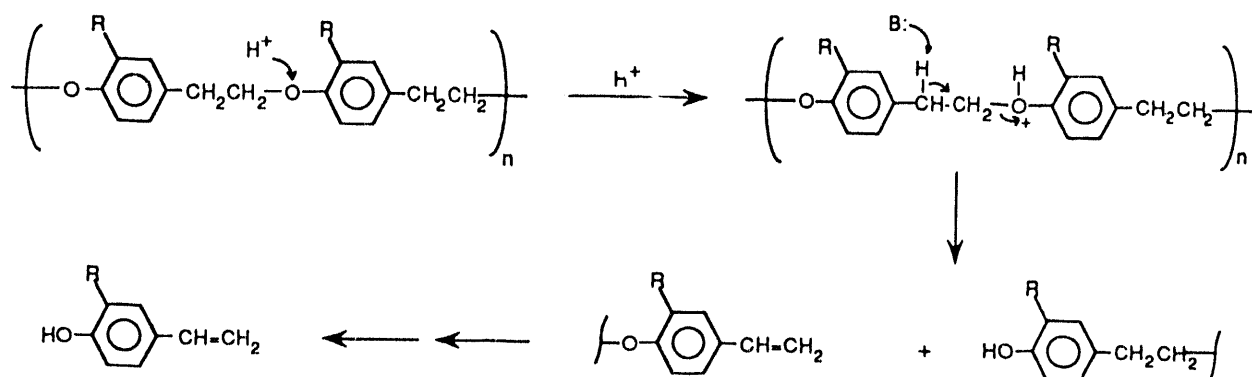
b. From Reference 31.

Consideration of the relative effects of the methoxy substitution on the initiation and propagation reactions (Table 7) reveals that the ortho-methoxy substitution should increase the rate of initiation and decrease the rate of propagation, changes which would tend to make the behavior less, not more, autocatalytic. That is, faster initiation without faster propagation would lower the onset temperature of reaction, but decrease the steepness of the second vaporization curve in Figure 6. The estimates in Table 7 are based on studies of the monomeric prototype itself (phenylphenethyl ether) by Klein and Virk (21), Gilbert and Gajewski (22), and Britt and Buchanan (23,31), as reviewed by Poutsma, (24,32) and the studies of bond-strength variations in substituted phenyl ethers and ethylbenzenes by Stein (28,29).

Another reason for being dissatisfied with an extension of the H-abstraction/ β -scission pathway of PPE is that a substantial amount of Ar-C bond scission also occurs with the H-substituted polymer, but is greatly suppressed by o-OMe substitution, as can be seen from the low intensity of the peak for methyl catechol (guaiacol, m/z 124) in Figure 9. This Ar-C cleavage is a reductive cleavage, taking place either by proton- or H-atom attack on the position bearing the Ar-C connection. Since H-atom attack (either free H-atom or H. transfer from a carrier species) should not be substantially affected by substitution meta- to the position of attack, but H⁺ or other electrophile attack would be suppressed, we tentatively conclude that the Ar-C cleavage is primarily the result of H⁺ attack on the aromatic ring. Further consideration of this "adjunct" and apparently electrophilic Ar-C bond scission allows us to propose an ionic, phenol-catalyzed depolymerization process that also provides a better explanation of the polymer decomposition behavior than any free radical pathway we have been able to devise. Thus, if electrophilic attack in the decomposing polymer is occurring at an aromatic carbon atom, then electrophilic attack at the inherently more basic ether oxygen needs also to be considered. The three major probable outcomes of such attack on ether oxygen are discussed below.

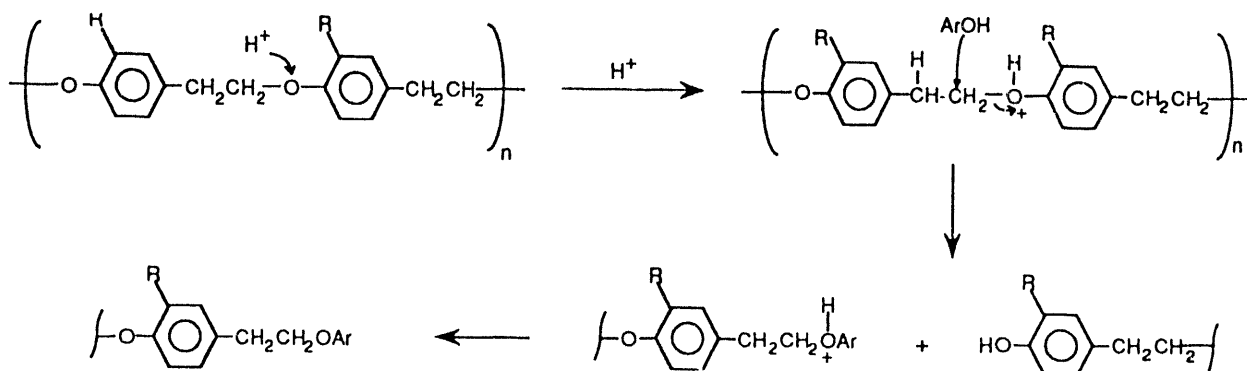
Electrophilic attack on the ether oxygen will in fact be coupled with nucleophilic attack: either on the α -carbon, or on the β -hydrogen. Bimolecular nucleophilic attack on the α -carbon, which in this polymer system would probably be by a phenolic molecule, releases a phenol and generates a new ether

linkage (Scheme 4). While this reaction might well occur, it would simply convert one ether to another, and would not necessarily result in molecular weight reduction.



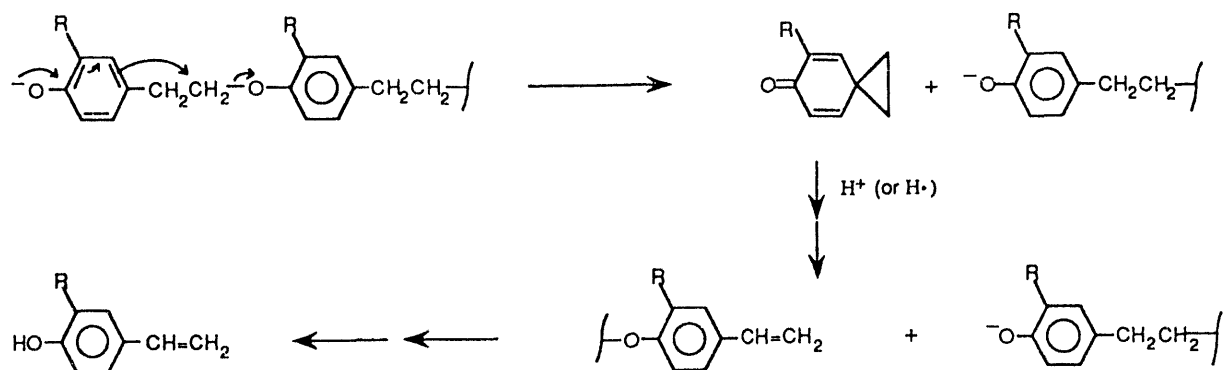
Scheme 4. Possible decomposition sequence involving acid-catalyzed ether cleavage of -O-C-C- polymers.

Furthermore, it is not obvious how this attack would result in more facile reaction at the ether linkage adjacent to a free phenol. Base attack on the β -hydrogen would generate the observed products, oligomers with a phenolic termination on one end and a vinylbenzene termination on the other (Scheme 5). However, this reaction should not be significantly promoted by the presence of a free -OH at the para position.



Scheme 5. Possible decomposition sequence involving acid-catalyzed attack on the ether oxygen coupled with base attack at the β -hydrogen.

On the other hand, if H^+ attack at the ether oxygen were coupled with base attack at the adjacent free OH, then an internal nucleophilic displacement is possible, forming a spiro-ketone and displacing a phenoxy anion (Scheme 6). This would provide a true unzipping process, would explain autocatalysis by phenolic products, and would be consistent with suppressed Ar-C bond cleavage in the methoxy substituted polymer. At the temperatures of interest here, the spiro-ketone would quickly ring open to give the vinylaromatic termination we observe.



Scheme 6. Possible decomposition sequence involving acid-catalyzed attack on the ether oxygen coupled with base attack on the free phenol termination.

O-Methyl Cleavage and Trans-Methylation during Pyrolysis. The Py-FIMS spectrum of the -OMe substituted polymer also shows substantial levels of satellite peaks at $\pm n(14)$ mass units from each of the main oligomer peaks (compare Fig. 9 with Fig. 8). Qualitatively, this is expected, since the ArO-Me bond is relatively weak. Furthermore the O-Me bond is weakened another 3 kcal/mol (see Table 7) by conversion of the ortho- -OCH₂CH₂ linkage to an -OH group, (28) increasing the bond homolysis rate at 350°C by slightly more than a factor of 10. Thus, one would not expect the O-Me bond scission to be random, but to occur preferentially at the terminal unit in a chain. Examination of the spectrum in Fig. 9 reveals that this is exactly what happens. The intensity of satellites at -14 Daltons increases, but from roughly 20% of the main oligomer peak in the monomer to only about 40% of the main peak in the hexamer. This two-fold increase is much less than the roughly six-fold increase that purely statistical cleavage would dictate. The observation of rather little methyl loss, except from the terminal unit, means that notwithstanding its moderately weak connection to ArO-, most of the O-Me aralkyl ether "caps" in a methylated coal should, under appropriate conversion conditions, remain intact long enough to provide some crosslink protection for dihydroxyaromatic units.

Hydrogen Balance during Pyrolysis. The aryl-carbon cleavage discussed above, regardless of whether it proceeds through displacement of a -CH₂CH₂O-Aryl unit by proton transfer or by H-atom transfer, constitutes a reduction reaction. Furthermore, the FI mass spectra in Figs. 8 and 9 show significant intensity at ± 2 Daltons from each of the main and transalkylated oligomer peaks. The ultimate origin of the hydrogen necessary to form the dealkylated or otherwise reduced oligomers is not evident in the mass spectra of Figs. 8 or 9. For example, in Fig. 8, the sum of hydrodealkylated and reduced oligomers, at least up to $n = 4$, is about ten times the sum of oxidized oligomers. Presumably the necessary additional hydrogen has come from char formation, i.e., from the 15% of the $-\text{[PhCH}_2\text{CH}_2\text{O]}_n-$ that failed to volatilize under the pyrolysis FIMS conditions. Such disproportionation phenomena are quite common in pyrolytic processes, such as the hydrotreating of petroleum- or coal-derived resids, although the detailed mechanisms have never been elucidated (33).

Retrograde Reactions. The small amount of char formation observed in the Py-FIMS and TG-FTIR of $-\text{[C}_6\text{H}_5\text{CH}_2\text{CH}_2\text{O]}_n-$, as referred to above in the discussion of hydrogen balance, indicates retrograde reactions are not very pronounced, at least in the basic, linear polymer. We expected that the tendency toward crosslinking would become more pronounced in the ortho-methoxy substituted polymer, which contains the dihydric phenol structures known (34) to be more susceptible to coupling reactions (and presumably is another step closer to actual low-rank coal structures). However, the TGA weight-loss data and FIMS vacuum vaporization curves show no increased tendency toward retrograde reactions with the ortho-methoxy substituted polymer (Table 6). To test the possibility that the methyl ether is "protecting" the second hydroxyl group in the $-\text{[C}_6\text{H}_3(\text{o-OMe})\text{CH}_2\text{CH}_2\text{O]}_n-$ polymer from crosslinking reactions, and to compare the results of methylating hydroxyl groups in a C-C-O-linked polymer with the impact of methylating real coals (13), we used the conditions described in the

experimental section to generate a polymer having about 45% of the ortho-substituents as free hydroxyl groups. This polymer with "de-protected" hydroxyl groups showed surprisingly little difference in behavior from the fully methylated polymer, exhibiting similar T_{max} values, volatiles yields, and oligomer distributions, as shown above in Table 6. The surprisingly low level of retrograde reaction in these highly oxygenated polymers is presumably due to relatively rapid removal of volatile products under either the vacuum conditions of FIMS or the flowing He (1 atm) of the TG-FTIR, to the fact that there are no original crosslinks in these polymers, or perhaps because some important coupling partners present in real coals are lacking here. Thus increasing the confinement during conversion (i.e., moving from pyrolysis to liquefaction) is an appropriate next step. It is not clear, a-priori, whether the increased confinement will outweigh the presence of a hydrogen donor and result in significant retrogression under liquefaction conditions. The next step following this would be to introduce some crosslinks into the original linear polymers. Ideally this could be done with a minimum of further synthetic effort via radiolytic crosslinking procedures that are used commercially for polystyrene and other polymers.

The Behavior of Carboxyl Functions in a Coal Liquefaction Environment

Introduction - Coupling reactions resulting from decarboxylation have long been associated with the retrograde reactions that hinder the pyrolysis and liquefaction of low-rank coals. However, examination of the literature on decarboxylation of aromatic and aliphatic carboxylic acids and on carboxyl functions in coal made it clear that additional examination of the thermal behavior of the carboxylic and phenolic functions in coal-related monomeric systems was necessary not only to understand how decarboxylation-promoted coupling might be occurring in coal, but is necessary even to make relevant choices of polymer and carboxyl function types for the study of decarboxylation and crosslinking in polymeric model systems. Carboxyl functions have been implicated in the crosslinking of coals at relatively low temperatures (11), and Solomon and coworkers (13) have been able to model the pyrolytic loss of solvent swelling by including one additional crosslink in the network for every CO_2 evolved. Moreover, pretreatments that have been found to be effective in promoting liquefaction, have also shown a corresponding decrease in the early CO_2 evolution (35). These results strongly suggest that carboxyl functions are involved in the low-temperature crosslinking of coals. However, the chemical reactions linking decarboxylation with coupling have not been delineated. In a recent study, Siskin and coworkers (41) showed that decarboxylation of naphthoic acid under hydrothermal conditions was attended by some binaphthyl; however, the coupling aspect was not elaborated in that study. In the current work, the literature was examined and over 40 experiments were conducted with monomeric aromatic and aliphatic carboxylic acids in organic media to see if crosslinking results directly from decarboxylation, and how crosslinking may be affected by ion exchange, the presence of a hydrothermal environment, and other conditions relevant to pretreatments that are being tested in this project.

Examination of the literature on decarboxylation (37-40), as well as earlier results obtained at SRI on decarboxylation under coal liquefaction conditions (41), allow us to make the generalization that coupling is not typically a widespread result of decarboxylation (except for the "dry" pyrolysis of alkaline earth salts of aliphatic carboxylic acids (39,40)). Thus, it is critical to choose appropriate structures and conditions for decarboxylation of coal relevant polymeric models. Moreover, limited coupling reported in the literature suggests that there is reasonable hope for finding coal liquefaction (or pretreatment) conditions that significantly decrease any coupling that results from decarboxylation. In the following subsections, the results of the decarboxylation experiments performed in this project are discussed. In the summary, a somewhat broader discussion of decarboxylation is presented as it applies to coal liquefaction, using information drawn from these recent experiments as well as from earlier SRI work and data in the literature.

The Decarboxylation of Activated and Unactivated Benzoic Acids - The carboxylic acids shown in Table 8 have been subjected to "liquefaction" conditions and the products analyzed by gas chromatography to determine the extent of decarboxylation and coupling that resulted.

The data in this table demonstrate that the decarboxylation of benzoic acid itself is slow at 400 °C in tetralin (3-5% in 1 hr), unless a fairly strong base or other decarboxylation promoter is present. Surprisingly, the decarboxylation of calcium benzoate in tetralin is no faster than that of the free acid. With respect to coupling, we see that when decarboxylation is promoted by bases, there is little or no evidence for coupling, either with benzene, tetralin, naphthalene, or even the very good acceptor,

Table 8. Decarboxylation of Activated and Unactivated Benzoic Acids

Acid Structure	Solvent System	Concentration m%	Reaction Time Hrs	% Decarboxylation	% Coupling ¹
PhCO ₂ H ^{2,3}	Tet/THQ ⁴ 75/20	5	1	4	<20
	Tet/THQ/H ₂ O 55/20/20	5	1	5	<20
	Tet/PipPy 75/20	5	0.5	77	<3
	Tet/THQ/Zn(OAc) ₂ ⁷ 5/20	5	1	75	<5
	Tet/1-Naphthol 80/10	10	1	3	<2 ⁵
	Ca(PhCO ₂) ₂	Tet/1-Naphthol 80/10	10	1	3
4-OH-PhCO ₂ H	Tet	10	1	>98	<10
1-OH-PhCO ₂ H	Tet	20	1	>99	<5
3-OH-PhCO ₂ H	Tet	10	1	2	-
2-OMe-PhCO ₂ H	Tet	10	1	>98	<3
	Tet	20	1	>99	<3
	Tet/Pyrene	10	1	>99	<3
3-OMe-4-OH- PhCO ₂ H	Tet	10	1	>99	<2
3-OMe-4-OMe- PhCO ₂ H	Tet	10	1	~75	<3

1. This figure should be considered an upper limit; it represents the sum of small unidentified high mass peaks that are potential coupling products, given as a percent of decarboxylation. Thus larger values listed for cases where there is limited decarboxylation do not generally reflect larger absolute amounts of possible coupling products.
2. The first four sets of data for benzoic acid itself are taken from previous work.
3. For economy of space, the symbol "Ph" is used here to represent a single phenyl ring, regardless of whether there are 3, 4 or 5 unsubstituted positions on the ring.
4. "THQ" represents 1,2,3,4-tetrahydroquinoline, "Tet" is tetralin, and "PipPy" is the strong organic base/nucleophile 4-Piperidinopyridine.
5. Does not include formation of naphthylbenzoate ester or rearranged product of this ester.

pyrene. This absence of coupling, together with the slow decarboxylation of benzoic acid itself at 400°C, raises the question whether unactivated aromatic carboxylic acids actually represent the acid species that undergo facile decarboxylation between 250 and 350°C during the heating of low-rank coals. Therefore, additional experiments were chosen to examine the behavior of benzoic acid derivatives known (37,38) to be activated toward decarboxylation via electrophilic attack. The ortho- and para-substituted acids listed in Table 8 were tested. For all of these, except for the meta hydroxy acid and veratric acid (3-OMe-4-OMe-C₆H₃CO₂H, last row in Table 8, decarboxylation in tetralin was complete in one hour at 400°C. Again however, there was no substantial level of coupling products. Even counting the sum of small, unidentified peaks that sometimes appear at high retention times, the total coupling amounts, at most, to 5% of the decarboxylated acid.

The mechanism of decarboxylation of these activated acids is not as clear as the literature (37,38) might suggest. For instance, veratric acid, the only one of the activated acids not possessing a free phenolic OH, did not undergo complete decarboxylation, but was recovered in ca. 25% yield after 1 hour in tetralin at 400 °C. This result is in contrast to the analog containing a free -OH in the same position, which underwent complete decarboxylation. Because *p*-OMe is generally just as activating toward electrophilic attack as *p*-OH, the above difference indicates that the rate determining step cannot simply involve attack on the starting material itself. That is, this result suggests that the principal mode of decarboxylation by electrophilic attack either involves reaction of the phenoxy anion or the keto form of the phenolic acid, which is accessible only through the free phenol. A third alternative, namely that the keto form might simply undergo thermal unimolecular bond cleavage (homolysis) to give phenoxy and •COOH, radicals is analogous to cleavage described in the literature (41) for benzylphenols and phenoxyphenols, but can be ruled out here because the instability of the •COOH radical makes its formation too endothermic. This uncertainty about a decarboxylation whose mechanism was supposedly understood simply emphasizes that few definitive statements about decarboxylation-promoted coupling can be made without further experimental work.

The uncertainty of decarboxylation mechanisms notwithstanding, we identified certain changes in substrate-structure/reaction-conditions that should made decarboxylation experiments more relevant to the conditions that actually prevail during liquefaction and also more likely to facilitate coupling, while yet remaining simple enough to provide chemical understanding.

Conditions likely to promote coupling in conjunction with decarboxylation: 1) increased concentration and/or improved coupling partners (such as polycyclic aromatic hydrocarbons for aryl radicals); 2) decreased concentration of radical scavengers; 3) electron-transfer agents that may convert carboxylate anions to radicals, which then decarboxylate to yield aryl radicals; 4) conversion of the acids to their Ca or Mg salts, forms known in the coals themselves to increase char formation, and in alkane carboxylic acids (40) to yield ketone coupling products; 5) addition of structures that may couple by forming electrophilic agents that attack the acids themselves, rather than merely react with aryl radicals produced in decomposition of the acids. Item 1 has already been partially addressed with several of the experiments listed in Table 8, and did not result in significantly increased coupling. Items 2 through 5 are dealt with in considerable detail in the experiments described in the sections that follow.

Effect of Calcium Salts - The calcium salts of benzoic acid and anisic acid were prepared, purified, and tested, both in a poor "liquefaction" medium and neat. In brief, the results are that the decomposition of the calcium salts does *not* substantially increase the tendency for crosslinking to occur in association with decarboxylation. This behavior is in contrast to the apparent behavior of ion-exchanged low-rank coals (2,10,11,17) and in contrast to the known behavior of neat salts of aliphatic carboxylic acids (39,40).

The Effect of Electron-Transfer Agents and the Acceptor/Scavenger Ratio - Because of the low levels of coupling products observed in the experiments described above, where we attempted to grossly simulate the donor solvent environment of liquefaction by using tetralin or tetralin mixtures as the reaction medium, most of the remaining experiments in this study were performed in more oxidizing systems, i.e., without either hydro- or alkyl aromatic species in the mixture. Under these conditions, literature data for the reactions of phenyl and other aryl radicals lead one to expect that any phenyl radicals formed will add very readily to essentially any aromatic system, displacing hydrogen to form biaryl linkages. However, since naphthalene is a better radical acceptor than benzene, we used it as

the dominant component of most reaction mixtures to further increase the chances of forming coupling products from any aryl radicals that are generated. Accordingly, we have allowed benzoic acid to react (at 400°C) in the presence of varying amounts of naphthol, naphthalene, and methylnaphthalene, as well as tetralin, and have used pyridine and the calcium salt of benzoic acid as bases, and Fe₃O₄ and Cu(OAc)₂ as electron-transfer agents. The major differences between these two one-electron transfer agents are illustrated by the data in Table 9.

Table 9. Effects of Different 1-Electron Oxidants on Coupling and Decarboxylation of Benzoic Acid During Reaction at 400°C for 1 Hour

Exp.	Reactants (mol%) ^a					Results				
	BA	Naphth.	Pyridine	Fe ₃ O ₄	Cu Acet.	%Unr. Acid	% Ph-Naph ^b	% Py-Naph ^b	% Binaph. ^b	% Decarbox. ^c
1	11.3	68.8	9.8	10.1	—	19.5	3.2	2.93	2.66	57.3
2	10.4	70.4	8.9	—	10.3	< 0.1	0.28	0.65	2.03	83.4

^a BA = benzoic acid; Naphth. = Naphthalene; Cu Acet. = Cupric Acetate monohydrate [Cu(CH₃CO₂)₂·H₂O].

^b Ph-Naph = 1 and 2-phenyl naphthalene; Py-Naph = pyridinylnaphthalenes; Binaph. = binaphthalenes. Results are given as a mol% of the starting *benzoic acid*. It has thus been assumed that pyridinylnaphthalenes and binaphthalenes are coupling products that stem from decarboxylation after a shift of the radical center from the initial phenyl radical to either pyridine or naphthalene. This assumption is being checked and could be incorrect.

^c Based on identified decarboxylated products including benzene and phenyl-containing coupling products.

Both agents markedly increase decarboxylation (from 3-5% as shown in Table 8 to at least ~60% as seen in Table 9). Decarboxylation rates are at least ten times faster with Cu(OAc)₂ than with Fe₃O₄, but the coupling is about ten times faster in the presence of Fe₃O₄. For present purposes, the results can be summarized as follows. The combination of pyridine and cupric acetate did enhance decarboxylation substantially, as the literature (37,38) indicates it should. However, we still see only very low levels of coupling products (other than ester formation from benzoic acid and naphthol, when it is present). Furthermore, we see this lack of substantial coupling even when we have replaced most or all of the tetralin with naphthalene to provide more good acceptors for phenyl radicals and to decrease the scavenging ability of the system. Under these latter conditions, reported phenyl radical H-abstraction (from tetralin) and aryl radical addition rates (42-44) suggested that the addition should definitely not be overwhelmed by scavenging of the phenyl radicals. Thus, from the data in Tables 8 and 9, it is still far from evident what chemical factors are here not allowing substantial coupling, but which may still allow such coupling during coal conversion.

After a few experiments with Cu(OAc)₂ and the mixed iron oxide Fe₃O₄, we decided to focus on Fe₃O₄ because (1) coupling was greater with iron oxide and the parameters affecting it could be more readily explored, (2) iron is more coal-relevant than copper and (3) decomposition of the acetate led to unwanted buildup of non-condensable gases (presumably methane) and perhaps distorted chemistry because of the demand of methyl radicals for hydrogen. Iron sulfides and iron sulfates are of course also relevant, but we have, for the time being, confined our iron-promoted decarboxylation studies to Fe₃O₄ in order to address the impact of changing the organic structural parameters.

The decarboxylation products observed in the presence of an added electron-transfer agent show the same isomer distribution observed in the absence of these agents. In the case of Fe₃O₄, the extent of coupling is increased dramatically. Thus, for this additive, the expected oxidation of the carboxylate anion to the carboxylate radical, which then rapidly decarboxylates, seems to be confirmed.

The Effect of Iron Oxide and Base on Coupling - The four experiments in Table 10 show the separate and combined impacts of iron oxide and pyridine on decarboxylation and coupling. All of the coupling product distributions above are listed in this table, but the major points are contained in the first four rows, where the reactant identities and concentrations are listed, and the last two rows, where the percent decarboxylation and the percent of decarboxylation that leads to coupling are shown. It can be seen that the conditions strongly affect both the amount of decarboxylation and the degree of coupling. In naphthalene only (Condition 1), benzoic acid undergoes about 4.4% decarboxylation and only 2.7%

Table 10. Effect of Fe₃O₄ and Pyridine on Decarboxylation and Coupling of Benzoic Acid During Reaction in Naphthalene at 400° C for 1 Hour

Reactants	Experiment							
	Condition 1		Condition 2		Condition 3		Condition 4	
	mmol	mol%	mmol	mol%	mmol	mol%	mmol	mol%
Benzoic Acid	0.1957	9.57	0.2031	10.00	0.2064	10.13	0.2260	11.26
Naphthalene	1.8499	90.43	1.6299	80.23	1.6205	79.49	1.3810	68.80
Pyridine	—	—	0.1985	9.77	—	—	0.1972	9.82
Fe ₃ O ₄	—	—	—	—	0.2116	10.38	0.2030	10.11
Products								
Benzoic Acid	0.19999	102.19	0.18803	92.58	0.20587	99.74	0.0440	19.48
Naphthalene	1.84617	99.80	1.62816	99.89	1.5943	98.38	1.3269	96.08
Pyridine	—	—	0.15658	78.88	—	—	0.1726	87.54
Benzene	0.00833	4.26	0.03671	18.07	0.01336	6.47	0.1223	54.11
Naphthalene Impurities	0.01425	0.77	0.01243	0.76	0.01214	0.75	0.01051	0.76
Biphenyl ^a	< 0.00004	< 0.004	< 0.00004	< 0.004	< 0.00004	< 0.004	0.00031	0.14
1-Phenylnaphthalene ^a	0.00011	0.058	0.00048	0.23	0.00488	2.36	0.0050	2.20
2-Phenylnaphthalene ^a	0.00011	0.055	0.00041	0.20	0.0021	1.02	0.0022	0.99
1-Pyridinylnaphthalene ^a	—	—	< 0.00004	< 0.004	—	—	0.0048	2.45
2-Pyridinylnaphthalene ^a	—	—	< 0.00004	< 0.004	—	—	0.0018	0.90
1,1'-Binaphthalene ^a	< 0.00004	< 0.004	< 0.00004	< 0.004	0.00093	0.905	0.00089	0.79
1,2'-Binaphthalene ^a	< 0.00004	< 0.004	< 0.00004	< 0.004	0.00149	1.440	0.0016	1.44
2,2'-Binaphthalene ^a	< 0.00004	< 0.004	< 0.00004	< 0.004	0.00046	0.441	0.00049	0.43
% Decarboxylation ^b		4.4		18.5		9.9		57.6
% (Coupling/Decarbox.) ^{b,c}		2.7		2.3		48.5		12.8

^a Mol percentages are based on the benzoic acid reactant. ^b Based on identified products. ^c It is assumed that pyridinylnaphthalenes and binaphthalenes are coupling products that stem from decarboxylation after a shift of the radical center from the initial phenyl radical to either pyridine or naphthalene (see text).

of the decarboxylated material is found as the coupling product phenylnaphthalene. The addition of pyridine base (Condition 2) increases decarboxylation by a factor of four, but the fraction of decarboxylation that leads to coupling products is unaffected, remaining at $2.5 \pm 0.2\%$. These results are consistent with a mechanism where decarboxylation involves primarily the carboxylate anion itself. To the extent that phenyl anion is the initial product of decarboxylation, its strong basicity seems likely to have it abstract a proton rather than couple with another molecule. The effect of base is then to increase the concentration of the benzoate anion and hence the rate of decarboxylation. The product is still phenyl anion, however, and the rate of coupling is therefore unaffected.

Substantial coupling is seen only in those systems where the 1-electron oxidant Fe_3O_4 has been added (Conditions 3 and 4). By itself, the addition of Fe_3O_4 leads to a factor of 2.5 increase in the rate of decarboxylation when compared with the naphthalene-only system. More significant, however, is the fact that now nearly one-half of the decarboxylated material is found as a coupling product.

When both pyridine and Fe_3O_4 are added (Condition 4), the degree of decarboxylation increases to about 60%. However, the fraction of decarboxylated material that couples is only 12.8%, a factor of 3.8 lower than with Fe_3O_4 only, but a factor of 5 greater than with no added Fe_3O_4 . Apparently the base directly or indirectly facilitates the transfer of a hydrogen to phenyl radical before it can couple. Notice that this effect of added base in suppressing the fraction of decarboxylation that leads to coupling was not observed in the absence of Fe_3O_4 (compare the results for Conditions 1 and 2), consistent with the supposition that, in the absence of Fe_3O_4 , the bulk of the decarboxylation goes through a different species. Although these observations on the effect of the base are, at present, not fully understood, they obviously could have ramifications with regard to the design of a system which minimizes coupling reactions in coal liquefaction.

The Effect of FeS - Because of the pronounced increase in decarboxylation-promoted coupling of benzoic acids brought about by the presumed electron-transfer agent, Fe_3O_4 , it was of interest to determine the impact of FeS, whose non-stoichiometric character might give it similar potential for promoting coupling.

The addition of FeS to benzoic acid in naphthalene increased the decarboxylation (during 1 hr at 400°C) from 4.5% to 45.5%. However, the coupling (to phenylnaphthalene, expressed as a % of the decarboxylation that yielded coupling) increased only from 2.5% to 5.7%. The increase in decarboxylation is several times greater than that observed with Fe_3O_4 , but the increase in coupling to about 6% is much less than the ~50% seen with Fe_3O_4 . Thus the principal general conclusion to be drawn from the relative impact of FeS is that the lower iron sulfides, which have long been known to have a net benefit on liquefaction, are not likely to be a cause of retrograde reaction during coal heating.

The Effect of Water - Because water has figured prominently in various coal pretreatment studies and because it has been shown to inhibit the coupling of phenolic structures, 10 mol% water was added to the system which has so far shown the greatest coupling (as a fraction of decarboxylation), namely the benzoic acid-naphthalene- Fe_3O_4 system. In the this case, however, there was no significant impact of water, either on decarboxylation or on coupling.

The Effect of H-Donors - As described above, H-donors were commonly absent from the reaction mixtures in an attempt to produce enough coupling products so that the factors affecting their formation could be readily studied. Table 11 shows that the replacement of roughly half of the naphthalene with the H-donor tetralin decreased not only the fraction of the decarboxylation that eventually led to coupling, but also the extent of decarboxylation.

Table 11. Effects of Solvent H-Donating Ability on Coupling and Decarboxylation of Benzoic Acid During Reaction at 400°C for 1 Hour in Presence of Base and the Electron Transfer Agent Cupric Acetate

Exp.	Reactants (mol%) ^a						Results			
	BA	Naphth.	Tet/MN	Pyridine	Naphthol	Cu Acet.	%Unr. Acid	% Coupling ^b	% Decarbox. ^c	%(Coup/Decarb)
1	9.8	—	58.8	12.2	9.6	9.7	45.9	0.51 ^d	46.5	1.1
2	10.4	70.4	—	8.9	—	10.3	<0.1	2.96	83.4	3.5

^a BA = benzoic acid; Naphth. = Naphthalene; Tet/MN = 50:50 mol/mol mixture of tetralin and 1-methylnaphthalene; Naphthol = 1-naphthol; Cu Acet.= Cupric Acetate monohydrate [Cu(CH₃CO₂)₂·H₂O].

^b Results are given as a mol% of the starting benzoic acid and refer to all peaks in the coupling region of the chromatogram.

^c Based on identified decarboxylated products including benzene and phenyl-containing coupling products.

^d This figure does not include 1% formation of naphthyl benzoate from benzoic acid and naphthol.

As discussed above, it was expected that the H-donor, functioning in its radical scavenger mode, would scavenge a larger fraction of the phenyl radicals before they could couple. However, it was not anticipated that the H-donor would also decrease the amount of decarboxylation, and this result cannot yet be rationalized. It would seem unlikely that an initially produced carboxyl radical would have a sufficiently long lifetime before decarboxylation to allow any significant scavenging by tetralin.

Effect of Fe₃O₄ on Decarboxylation of Activated Carboxylic Acids - In the absence of electron transfer agents, our previous results (discussed above) showed that coupling of activated acids was a very minor process under reductive coal liquefaction conditions. However, because of the large effect of Fe₃O₄ on the coupling products that were observed with benzoic and phenylacetic acid, it was thought to be important to examine the behavior of the activated acid o-anisic acid (2-methoxybenzoic acid) in the presence of this electron transfer agent.

As shown in Table 12, Fe₃O₄ promotes the formation of xanthenes from anisic acid. The last two experiments in the table show that the phenol and cresol generated as decarboxylation products are responsible for the formation of xanthenes. The self-coupling of cresol gives methylxanthene, while the cross-coupling of phenol and o-cresol give xanthene itself. The mechanism of Fe₃O₄-promoted xanthene formation most likely involves oxidation of the benzylic radical formed from o-cresol to the corresponding cation, which then should rapidly attack phenol or cresol, which are activated to electrophilic attack.

We had speculated, in the early stages of this study, that electrophilic agents, such as the ortho-hydroxybenzyl cation, might attack activated aromatic acids directly, to give coupling products that were formed in the very act of decarboxylation itself, not subsequent to it. Here we are seeing a third alternative, namely attack on activated species that are the products of decarboxylation but are not the radical or ion intermediates of the decarboxylation itself. Observation of these products makes it apparent that decarboxylation of activated acids to produce phenol-, cresol-, and catechol- derivatives, all of which are more activated toward electrophilic attack than the acids that gave rise to them, could be an important sequence for coals: retrograde reaction would be a result of decarboxylation, but the various decarboxylation intermediates themselves (i.e., radicals or ions), which we have found in most cases to yield very few coupling products, would not be the species directly involved in the coupling.

Decarboxylation of Phenyl-Substituted Alkane Carboxylic Acids - Since the distribution of carboxylic acid types in these coals is not known, and since the oxidation of non-benzylic alcohol carbons in the original lignin structure to aliphatic carboxylic acids is an alternative to oxidation of benzylic carbons to substituted benzoic acids, we have also performed experiments with phenylacetic acid. Table 13 shows that the decarboxylation of this aliphatic acid, which in tetralin alone is about six times higher than it is for benzoic acid in tetralin alone, is also markedly accelerated by electron-transfer agent and base.

Table 12. Fe₃O₄ Induced Coupling of Decarboxylation Products of Anisic Acid

Exp	Reactants (mol %) ^a	Results (as a % of starting material)					
		%Unr. Acid	Anisol	PhOH ^d	o-Cresol	Xanth ^{a,b}	Me-Xanth ^{a,b}
1	o-AA/Naph/Fe ₃ O ₄ 12.8/77.7/9.9	<0.1	19.8	46.3	12.5	6.9	1.7
2	Cresol/Naph/Fe ₃ O ₄ 9.7/80.3/10.0	---	---	6.3	67.8	0.36	4.2
3	Cresol/PhOH/Naph/Fe ₃ O ₄ 8.0/8.2/75.5/8.3	---	---	81.7	73.9	4.6 ^c	2.1 ^c

^ao-AA = ortho-anisic acid (2-methoxybenzoic acid); Naph = Naphthalene; Cresol = ortho-Cresol, PhOH = phenol, Xanth = Xanthene; Me-Xanth = Methylxanthene (isomer undefined).

^bThese species stem from two units of phenylacetic acid; given percentages are twice the mol%.

^cGiven as a percentage of the sum of the starting phenols.

Table 13. Effects of Radical Scavenger and 1-Electron Oxidant on Coupling and Decarboxylation of Phenylacetic Acid During Reaction at 400°C for 1 Hour

Exp	Reactants (mol%) ^a	Results (as a % of starting PAA ^a)						
		%Unr. Acid	Toluene	BB+SB ^{b,c}	DPA ^{b,c}	Bz-Naph ^b	Ph-Naph ^b	%Coup./%Reaction ^d
1	PAA/Naph 10.9/89.1	57.1	27.2	0.41	5.6	0.047	0.065	13.3
2	PAA/Naph/Tet 11.1/77.9/11.0	65.0	27.3	<0.15	5.3	0.23	<0.05	15.8
3	PAA/Naph/Tet 9.9/20.5/69.6	72.3	21.1	<0.15	2.6	0.46	<0.05	11.0
4	PAA/Tet 10.3/89.7	67.2	19.7	<0.15	1.3	0.48	<0.05	5.4
5	PAA/Naph/Pyridine 9.8/79.0/11.2	61.3	31.6	0.39	5.1	0.052	<0.15	14.3
6	PAA/Naph/Fe ₃ O ₄ 9.8/79.9/10.3	34.7	35.7	7.2	5.5	3.3	2.4	28.2
7	PAA/Naph/Tet/Fe ₃ O ₄ 9.9/70.7/9.5/9.9	31.6	35.3	4.8	20.9	1.7	0.52	43.2
8	PAA/Naph/Tet/Fe ₃ O ₄ 9.9/44.5/35.6/10.0	35.2	32.7	2.5	23.8	1.1	0.17	42.5
9	PAA/Tet/Fe ₃ O ₄ 10.0/80.0/10.0	42.0	29.2	1.1	23.6	0.62	<0.05	43.7

^aPAA = phenylacetic acid; Naph = Naphthalene; Tet = Tetralin

^bBB = Bibenzyl; t-SB = trans-stilbene; Bz-Naph = 1 and 2-benzyl naphthalenes; Ph-Naph = 1 and 2-phenyl naphthalenes.

^cThese species stem from two units of phenylacetic acid; given percentages are twice the mol%.

^dBased on identified coupling products and unreacted phenylacetic acid.

The nature and extent of coupling products, from phenylacetic acid and the impact of changing reaction conditions on these products are shown in Table 13 and can be summarized as follows. The major coupling product is dibenzyl ketone, which is decreased from 5.6% (of decarboxylated acid) to 1.3% when the reaction medium is changed from naphthalene to tetralin. The addition of pyridine increases the decarboxylation slightly, but does not affect the fraction of decarboxylation that leads to coupling. The addition of Fe_3O_4 increases decarboxylation by about 30%, but increases by factors of 20 to 70 various minor coupling products (benzyl- and phenyl- naphthalenes, bibenzyl, and t-stilbene) that arise by radical addition reactions. This increase in coupling products formed via radical pathways is consistent with the behavior of Fe_3O_4 in the presence of aromatic carboxylic acids, namely to increase the oxidation of carboxylate anions to radicals and thereby to increase the yield of radical-induced coupling products.

In contrast, Fe_3O_4 has *no effect, in pure naphthalene*, on the fraction of decarboxylation that leads to dibenzyl ketone. However, when the naphthalene contains as little as 10% tetralin, Fe_3O_4 increases dibenzyl ketone by 300%. This impact of tetralin when Fe_3O_4 is present, is dramatically different from its effect in the absence of Fe_3O_4 , which is to suppress by ~80%, the formation of dibenzyl ketone! This dramatic effect of the combination of tetralin/ Fe_3O_4 is not presently understood.

Finally, the addition of water substantially suppressed the formation of dibenzylketone from phenylacetic acid. This supports our speculation that the acid anhydride and the phenyl ketene that is thermally generated from it are intermediates in the formation of dibenzyl ketone. If the last stage in dibenzyl ketone formation involved benzyl radical addition to phenylketene, then the successful formation of dibenzyl ketone could be critically dependent on this adduct acquiring a hydrogen atom from some scavenger.

SUMMARY AND CONCLUSIONS

The work in this project has involved three major areas of effort on: 1) coals and modified coals; 2) model polymers; 3) model compounds. Studies have been done to elucidate the role of oxygen functional groups in crosslinking and cleavage reactions. The work on coals and modified coals indicates that cation exchanged carboxyl groups promote crosslinking reactions in both pyrolysis and liquefaction systems and/or act as initial crosslink sites. The association of the coal moisture with cations can interfere with these cation effects. This phenomenon may explain why the thermal reactions of coal during the coalification process, where liquid water is present, follows a different pathway than open-system pyrolysis.

The model polymer systems with a β -ether linkage and different ring substituents showed similar pyrolysis behavior. The kinetics and mechanism of the decomposition were much different than would be expected based on studies of the analogous model compounds. The extent of retrogressive reactions was low in pyrolysis studies and the unzipping behavior exhibited during decomposition was more similar to lignin than low rank coals. This result may be due to one or more factors: a) the β -ether linkage is not common in low rank coals; b) the absence of carboxyl groups and dihydroxy functions; c) the absence of cations.

The work on model compounds illustrated the ability of oxygen functions like OH and OMe to influence the decomposition rates of other types of functional groups, such as carboxyl. This work also demonstrated that the amount of coupling resulting from the decomposition of carboxyl or carboxylate groups is strongly influenced by the reaction conditions and the presence or absence of electron transfer agents.

The specific conclusions for each area are summarized below:

Studies on Ion-Exchanged Coals - Preparation of ion-exchanged (including barium, calcium and potassium) demineralized Zap and Wyodak was done. Both vacuum dried and moist samples were prepared. The modified samples were subjected to functional group analysis as KBr pellets with FT-IR spectroscopy and programmed pyrolysis analysis with TG-FTIR. Liquefaction experiments of these samples were also performed and products were analyzed. The data show that both the pyrolytic tar and liquefaction yields decrease with the extent of ion-exchange, i.e., in the order of (demineralized) >

(ion-exchanged at pH 8) > (ion-exchanged at pH 12.5). The conclusions from this study are as follows:

- The addition of monovalent (K^+) or bivalent (Ca^{+2} , Ba^{+2}) cations to acid demineralized coals at pH 8 significantly increases the extent of retrogressive reactions in pyrolysis and liquefaction (liquid yields are reduced). The effect is even more pronounced at pH 12.5.
- The ability of cations to act as initial crosslinks in the coal structure through electrostatic or covalent interactions is believed to be an important aspect of their role in promoting retrogressive reactions.
- Since the moisture in low rank coals is associated with the cations, the presence of liquid water during pyrolysis (as in hydrothermal treatment) or liquefaction can help to mitigate these reactions.
- The total evolution of CO_2 and CO from pyrolysis is changed significantly by cation-exchange. However, only in the case of CO does the evolution profile change significantly.
- After careful demineralization, a calcium form Zap or Wyodak coal can be prepared at pH= 8, which is similar to the raw coal with regard to pyrolysis and liquefaction behavior.

Studies on Model Polymers - Three variations of $—[PhCH_2CH_2-O]_n—$ polymers exhibited similar pyrolysis results, rapidly depolymerizing in high yield at 350 to 400°C to a series of olefin-terminated oligomers. The volatiles yields were 83 to 87 wt% for all three polymer variations under one-atmosphere TG-FTIR conditions and 80 to 100% for under vacuum in Py-FIMS. This general behavior was expected, inasmuch as the simplest element of these polymers, phenylphenethyl ether, undergoes fairly rapid central bond cleavage in a radical-chain H-abstraction— β -scission process. However, the detailed behavior was quite surprising. The unexpectedly rapid, strongly autocatalytic, unzipping decomposition behavior indicate a depolymerization pathway different than the radical chain process known to account for the decomposition of phenylphenethyl ether. We suggest that the C-C-O linkage adjacent to the terminal para-OH group may react via an acid/base catalyzed process. The phenoxy anion, which can be generated only at the terminal unit, undergoes an internal nucleophilic displacement to form a transient intermediate spiroketone and eliminate a phenoxy anion on the decomposing chain. The spiroketone would rapidly ring-open to give the observed product *p*-hydroxy styrene.

The suggested depolymerization pathway of course needs to be verified. However, it can potentially account for the autocatalysis, the unzipping tendency, the unexpectedly rapid reaction, and the hydrodealkylation side reaction and its influence by -OMe ring substitution. *None* of these observations can be accounted for by the radical chain process that dominates for phenylphenethyl ether itself. The new mechanism could also account for the heretofore unexplained unzipping tendency of lignins and the susceptibility of low rank coals to promotion of liquefaction by base.

Studies on Model Compounds - The more important specific results of our studies with activated and unactivated aromatic carboxylic acids and one aliphatic carboxylic acid, phenylacetic acids can be summarized as follows.

- Simple benzoic acids (i.e., not substituted in the ortho- or para- positions with electron releasing groups) do not rapidly decarboxylate except in the presence of strong base and/or electron transfer agents.
- Upon decarboxylation, benzoic acids form only minor amounts (i.e., <5%) of coupling products, either with themselves or with aromatics that are part of the reaction system. Neither the absence of any nominal H-donor to scavenge any radicals formed upon decarboxylation, nor the addition of naphthol or pyrene, which are very good radical acceptors, substantially increase the yield of coupling products.
- The presence of Fe_3O_4 moderately promotes decarboxylation of unactivated aromatic acids and markedly increases (up to as much as 50%) the fraction of decarboxylation that leads to coupling with naphthalene. Water has no impact on this coupling.
- FeS and $Cu(OAc)_2$ promote decarboxylation, *without* any increase in the *fraction* of decarboxylation

that leads to coupling.

- Pyrolysis of calcium salts of activated or unactivated aromatic acids does not result in substantially faster decarboxylation or increased coupling.
- Pyrolysis, by themselves, of aromatic acids activated towards decarboxylation (e.g., o-anisic acid) results in only traces of coupling products, but the presence of Fe_3O_4 increases these products, including xanthene ring-coupling and ring-closure products, to about 10% of decarboxylation. The xanthene coupling products were shown to be generated from subsequent coupling of the cresol and phenol decarboxylation products, rather than from reactive decarboxylation intermediates.
- Pyrolysis of phenylacetic acid produces small amounts (1 and 6% in tetralin and naphthalene, respectively) of the coupling product dibenzylacetone, no analogs for which had been seen in the pyrolysis of aromatic acids. Added Fe_3O_4 had no impact on the coupling product in naphthalene, but in the presence of 10% or more tetralin it increased the yield of dibenzyl acetone by a factor of four.

The general implications and questions for decarboxylation-promoted retrograde reactions during coal liquefaction are as follows.

- Unactivated aromatic acids, because of their slow decarboxylation rates and low yields of coupling products are not good candidates for explaining retrograde reactions that in coal liquefaction are correlated with CO_2 formation.
- The electron-transfer agent Fe_3O_4 results in as much as 50% of benzoic acid decarboxylation going to generate coupling products, but the rate of decarboxylation was still too slow to account for the retrograde reactions that take place as low rank coals are still approaching liquefaction temperatures.
- Activated aromatic acids decarboxylate in the the right temperature region to account for the decarboxylation behavior of low-rank coals, but do not yield substantial amounts of coupling products. The major coupling products observed from anisic acid, a prototypical activated acid, were xanthenes, which were determined to arise not from radical or ion intermediates of the decarboxylation but from subsequent reaction of the phenolic decarboxylation products. This raises the question of whether the observed correlation between decarboxylation and retrograde reactions of coals might result from the fact that elimination of the carboxylic acid functionality from activated acids (producing substituted phenols and catechols) increases their degree of activation toward electrophilic coupling reactions.
- The behavior of phenylacetic acid, the only aliphatic acid tested in this study, suggests that aliphatic acids may be better candidates for explaining decarboxylation-promoted retrograde reaction of coals. We observe $\text{R-CO}_2\text{H}$ to produce $\text{R}_2\text{C=O}$ under liquefaction conditions, and the neat pyrolysis of alkaline earth salts of these acids is known to produce high yields of $\text{R}_2\text{C=O}$. The inhibition, by added water, of dibenzyl ketone formation is also consistent with coal liquefaction behavior.

REFERENCES

1. Bishop and Ward, *Fuel*, **37**, 191, (1958).
2. Schafer, H., *Fuel*, **49**, 197, (1970).
3. Hengel and Walker, *Fuel*, **63**, 1215 (1986).
4. Vorres, K.S., *Energy & Fuel*, **4** (5), 420 (1990).
5. Harrison, I.T., *J Chem. Soc. Chem. Commun.*, 616, (1969).
6. Carroll, J.F., Kulkowit, S., McKervey, M.A., *J. Chem. Soc. Chem. Commun.*, 507, (1980).
7. Serio, M.A., Kroo, E., Teng, H., Charpenay, S. and Solomon, P.R., First Annual Report for U.S. DOE Contract No. DE-AC22-91-PC91026 (1992).
8. Serio, M.A., Kroo, E., Teng, H., Charpenay, S. and Solomon, P.R., Fifth Quarterly Report, U.S. DOE Contract No. DE-AC22-91-PC91026 (1992).
9. van Bodegom, B., van Veen, J.A., van Kessel, G.M.M., Sinnige-Nijssen, M.W.A., and Stuiver,

- H.C.M, Fuel 63, 346 (1984).
10. Wornat, M.J., and Nelson P.F., Energy and Fuel, **6** (2), 136, (1992).
 11. Suuberg, E. M., Lee, D., Larsen, J. W., Fuel, **64**, 1668, (1985).
 12. Suuberg, E.M., Unger, P.E., and Lapsen, J.W., Energy & Fuels, **1**, 305, (1987).
 13. Solomon, P. R., Serio, M. A., Deshpande, G. V., Kroo, E., Energy Fuels, **4**, 42, (1990).
 14. Solomon, P.R., Serio, M.A., and Suuberg, E.M., Coal Pyrolysis: Experiments, Kinetic Rates, and Mechanisms, Progress in Energy and Combustion Science, **18**, pp 133-220, (1992).
 15. Schafer, H., Fuel, **51**, 4, (1972).
 16. Kroo, E., Bonanno, A.S., Serio, M.A., and Solomon, P.R., Proceedings of the International Conference on Coal Science, Banff, Alberta, Canada, September 12-17, pp 473-476 (1993).
 17. Serio, M.A., Kroo, E., Teng., H., Solomon, P.R., "The Effects of Moisture and Cations on Liquefaction of Low Rank Coals," ACS Div. of Fuel Chem. Prepr. **38** (2), 577 (1993).
 18. Ross, D.S., Hirschon, A., Tse, D.S., and Loo, B.H., ASC Div. of Fuel chem. Prepr., **35** (2), 352, (1990).
 19. Serio, M.A., Kroo, E., Charpenay, S., and Solomon, P.R., "Hydrous Pyrolysis of Four Argonne Premium Coals," ACS Div. of Fuel Chem. Preprints, **37**, (4), 1681, (1992).
 20. Landais, P., and Monthieux, M., Fuel Proc. Tech., **20**, 123, (1988).
 21. Klein, M.,T., Virk, P.S., Ind. Eng. Chem., Fundam, **22**, 35 (1983).
 22. Gilbert, K.E., Gajewski, J.J., J. Org. Chem., **47**, 4899 (1982).
 23. Britt, P., Buchanan, A.C., Energy and Fuels, **6**, 110 (1992).
 24. Poutsma, M.L., "A Review of Thermolysis Studies of Model Compounds Relevant to Processing of Coal," Oak Ridge National Laboratory Report, ORNL/TM-10637, (1987).
 25. Solomon, P. R., Serio, M. A., Carangelo, R. M., Bassilakis, R., Gravel, D., Baillargeon, M., Baudais, F. Vail. G., Energy & Fuels, **4**, 319 (1990).
 26. St. John, G. A., Buttrill, S. E., Jr., Anbar, M., in Organic Chemistry in Coal, J. Larsen, Ed., ACS Symposium Series 71, Washington, D. C., p.223 (1978).
 27. Evans, R. J., Milne, T. A., Energy & Fuels, **1**, 123 (1978).
 28. Suryan, M.M., Kafafi, S.A., Stein, S.E., J. Am. Chem. Soc., **11**, 4594, (1989).
 29. Stein, S. E., "Free Radicals in Coal Conversion in "Chemistry of Coal Conversion, R. H. Schlossberg (Ed.), Plenum Press, N.Y., pp 13-44, (1985).
 30. McMillen, D. F., Golden, D. M., Ann. Rev. Phys. Chem., **33**, 497 (1982).
 31. Britt, P. F., Buchanan, III, A. C. Hitsman, V. M. Am. Chem. Soc., Div. Fuel Chem. Preprints, **36**(2), 529 ,(1991).
 32. Poutsma, M.L., Energy & Fuels, **4**, 113, (1990).
 33. a. Savage, P. E., Klein, M. T., Kukes, S. G., Energy and Fuels, **2**, 619, (1988). b. McMillen, D. F., Manion, J. A., Malhotra, R. Am. Chem. Soc., Div. Fuel Chem. Preprints, **37**(4), 1636, (1992).
 34. McMillen, D. F., Chang, S.-J., Nigenda, S. E., Malhotra, R. Am. Chem. Soc., Div. Fuel Chem. Preprints, **30**(4), 414, (1985).
 35. Serio, M. A., Solomon, P. R., G. V., Kroo, E., Bassilakis, R., Malhotra, R., McMillen, D.F., Am. Chem. Soc. Div Fuel Chem. Prep., **35**(1), 61,(1990).
 36. Siskin, M., private communication, (1991).
 37. March, J., Advanced Organic Chemistry, 3rd Edition, John Wiley and Sons, New York, p 507, 562, 653, 842, 928, (1985).
 38. Cohen, T., Schambach, J. Am. Chem. Soc., **92**, 3189, (1970).
 39. Friedel, C. Justus Liebigs Ann. Chem., **108**, 122, (1958).
 40. Hites, R. A., Biemann, K. J., Am. Chem. Soc., **94**, 5772, (1972).
 41. McMillen, D. F., Ogier, W. C., Ross, D. S., J. Org. Chem., **46**, 3322, (1981).
 42. Fahr, A., Stein, S. E., J. Phys. Chem., **92**, 4951, (1988).
 43. Chen, R. H., Kafafi, S. A., Stein, S. E., Am. Chem. Soc., **111**, 1418, (1989).
 44. Fahr, A., Mallard, W. G., Stein, S. E., 21st Symposium International On Combustion: The Combustion Institute, 825, (1986).